



HAL
open science

On well-balanced implicit-explicit Lagrange-projection schemes for two-layer shallow water equations

Alessia del Grosso, Manuel J. Castro Díaz, Christophe Chalons, Tomás Morales de Luna

► **To cite this version:**

Alessia del Grosso, Manuel J. Castro Díaz, Christophe Chalons, Tomás Morales de Luna. On well-balanced implicit-explicit Lagrange-projection schemes for two-layer shallow water equations. 2022. hal-03655011

HAL Id: hal-03655011

<https://hal.science/hal-03655011>

Preprint submitted on 29 Apr 2022

HAL is a multi-disciplinary open access archive for the deposit and dissemination of scientific research documents, whether they are published or not. The documents may come from teaching and research institutions in France or abroad, or from public or private research centers.

L'archive ouverte pluridisciplinaire **HAL**, est destinée au dépôt et à la diffusion de documents scientifiques de niveau recherche, publiés ou non, émanant des établissements d'enseignement et de recherche français ou étrangers, des laboratoires publics ou privés.

On well-balanced implicit-explicit Lagrange-projection schemes for two-layer shallow water equations

A. Del Grosso*, M. Castro Díaz,[†] C. Chalons[‡] and T. Morales de Luna[§]

Abstract

This work concerns the study of well-balanced Lagrange-projection schemes applied to the two-layer shallow water system. In particular, a formulation of the mathematical model in Lagrangian coordinates is proposed. The HLL method is then applied to a simplified version of the resulting Lagrangian system. Furthermore, based on the acoustic-transport splitting interpretation, another approximate Riemann solver for the acoustic-Lagrangian step is described. Both an explicit and an implicit-explicit method are proposed, where the latter can allow very fast simulations in sub-critical regimes. Finally, we show numerical simulations in which the outputs are compared with the IFCP method's results.

1 Introduction and mathematical model

In this work we are interested in the numerical approximation of the 1D two-layer shallow water system, which models a fluid composed of two superimposed layers of immiscible liquids where the upper one has a smaller density ρ_1 . Thus, using the subscript $j = 1, 2$ to indicate the j th layer, we state $\rho_1 < \rho_2$. This kind of situations can occur when there are two liquids of different densities or even with a single fluid present at two different temperatures, as in oceanic flows. Referring for instance to [1, 3, 4, 5, 7, 18, 19] and also to figure 1 for the notations, the two-layer shallow water system is given by

*Université Paris-Saclay, UVSQ, CNRS, Laboratoire de Mathématiques de Versailles, 78000, Versailles, France. E-mail: alessia.delgrosso@ens.uvsq.fr.

[†]Dpto. de Análisis Matemático, Facultad de Ciencias, Universidad de Málaga, Campus de Teatinos S/N, 29081 Málaga, Spain. E-mail: mjcastro@uma.es

[‡]Université Paris-Saclay, UVSQ, CNRS, Laboratoire de Mathématiques de Versailles, 78000, Versailles, France. E-mail: christophe.chalons@uvsq.fr.

[§]Dpto. de Análisis Matemático, Facultad de Ciencias, Universidad de Málaga, Campus de Teatinos S/N, 29081 Málaga, Spain. E-mail: tmorales@uma.es

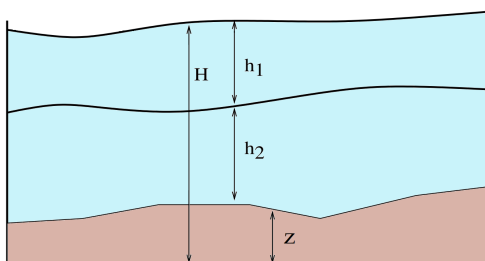


Figure 1: Sketch of the two-layer shallow water: h_1 , h_2 water heights, z topography and H free surface.

$$\begin{cases} \partial_t h_1 + \partial_x(h_1 u_1) = 0 \\ \partial_t(h_1 u_1) + \partial_x\left(h_1 u_1^2 + \frac{gh_1^2}{2}\right) + gh_1 \partial_x h_2 = -gh_1 \partial_x z \\ \partial_t h_2 + \partial_x(h_2 u_2) = 0 \\ \partial_t(h_2 u_2) + \partial_x\left(h_2 u_2^2 + \frac{gh_2^2}{2}\right) + g\frac{\rho_1}{\rho_2} h_2 \partial_x h_1 = -gh_2 \partial_x z \end{cases} \quad (1)$$

where $t > 0$ represents the time and x the axial coordinate. Then, $h_j(x, t) > 0$ is the water depth of the corresponding layer, $u_j(x, t)$ the averaged horizontal velocity and finally $z(x)$ the bed elevation. Regarding the parameters, we define the gravitational acceleration g and we shall denote $r = \frac{\rho_1}{\rho_2}$ the ratio of densities. These equations (1) can also be reformulated in a more compact way, namely

$$\partial_t \mathbf{Q} + \partial_x \mathbf{F}(\mathbf{Q}) + \mathbf{B}(\mathbf{Q}) \partial_x \mathbf{Q} = \mathbf{S}(\mathbf{Q})$$

where $\mathbf{Q} = (h_1, h_1 u_1, h_2, h_2 u_2)^T$ is the vector of unknowns,

$$\mathbf{F}(\mathbf{Q}) = \begin{pmatrix} h_1 u_1 \\ h_1 u_1^2 + \frac{gh_1^2}{2} \\ h_2 u_2 \\ h_2 u_2^2 + \frac{gh_2^2}{2} \end{pmatrix}, \quad \mathbf{B}(\mathbf{Q}) = \begin{pmatrix} 0 & 0 & 0 & 0 \\ 0 & 0 & gh_1 & 0 \\ 0 & 0 & 0 & 0 \\ rgh_2 & 0 & 0 & 0 \end{pmatrix} \quad \text{and} \quad \mathbf{S}(\mathbf{Q}) = \begin{pmatrix} 0 \\ -gh_1 \partial_x z \\ 0 \\ -gh_2 \partial_x z \end{pmatrix}.$$

Then, few computations show that the characteristic equation of the non-conservative matrix $\mathbf{A}(\mathbf{Q}) = \frac{\partial \mathbf{F}(\mathbf{Q})}{\partial \mathbf{Q}} + \mathbf{B}(\mathbf{Q})$ is given by

$$(\lambda^2 + u_1^2 - c_1^2 - 2\lambda u_1)(\lambda^2 + u_2^2 - c_2^2 - 2\lambda u_2) = rg^2 h_1 h_2$$

where by $c_j = \sqrt{gh_j}$ corresponds to the sound speed of each layer. In particular, it is easy to see that we have null eigenvalue when

$$G^2 = F_1^2 + F_2^2 - (1-r)F_2^2 F_1^2 = 1$$

where F_j such that $F_j^2 = \frac{u_j^2}{(1-r)c_j^2}$ are the internal Froude numbers and G is the composite Froude number, see also [18]. It is worth to specify that if $G^2 < 1$, we say to be in a sub-critical regime while $G^2 > 1$ indicates a supercritical flow. Depending on the value of r we may be able to explicitly define the eigenvalues of system (1) or not. Indeed, if $r = 0$, it is clear that the eigenvalues correspond to the shallow water system eigenvalues for each layer separately. Thus, if $r \approx 0$, the two layers of fluids behave almost independently. However, we are interested in situations in which $r \approx 1$, which often happen in geophysical flows. In this case, thanks to [21], the following first-order approximation of the eigenvalues are available

$$\begin{aligned} \lambda_{\text{Ext}}^{\pm} &= \frac{h_1 u_1 + h_2 u_2}{h_1 + h_2} \pm \sqrt{g(h_1 + h_2)} \\ \lambda_{\text{Int}}^{\pm} &= \frac{h_1 u_1 + h_2 u_2}{h_1 + h_2} \pm \sqrt{g_1 \frac{h_1 h_2}{h_1 + h_2} \left(1 - \frac{(u_1 - u_2)^2}{g_1 (h_1 + h_2)}\right)} \end{aligned}$$

where $g_1 = g(1-r)$ is the reduced gravity. It is a well-known fact that the two-layer system may lose its hyperbolic character and complex eigenvalues may arise. Indeed, in view of the first-order approximation of the eigenvalues, it is clear that the fulfillment of the following condition

$$\frac{(u_1 - u_2)^2}{g_1 (h_1 + h_2)} > 1$$

would lead to complex internal eigenvalues and thus we would lose the hyperbolicity of system (1). Physically speaking, this corresponds to situations where the mixing of the two layers would occur, leading to the appearance of shear instabilities. In practice, this mixture would partially dissipates the energy. To simulate such an effect, we could include friction in the mathematical model, otherwise in the numerical simulations the interface disturbances may grow and lead to a wrong solution [5]. Hence, it is clear that model (1) is not well-adapted to those situations and a more complex one would be needed. When we consider numerical tests, the lost of hyperbolicity could be accepted only in occasional situations to make sure we do not depart from the correct solution. For further informations about the two-layer shallow water model and its loss of hyperbolicity, see for instance [5, 4, 7].

Concerning the numerical strategy, here we aim to design and implement well-balanced implicit-explicit Lagrange-projection schemes. So far Lagrange-Projection (LP) methods have been studied for different mathematical models as the shallow water system [15] and related models [10, 11], the gas dynamic equations [13, 12] and the blood flow system [17]. However, up to our knowledge, they have never been employed to numerically approximate the two-layer shallow water equations. Indeed, due the presence of two velocities u_1, u_2 , it is not straightforward to understand how to apply the Lagrange-projection strategy to this system. Indeed, a first idea could be to implement the LP approach for each layer and then to couple them. However, it is known that a method that applies an arbitrary scheme to each layer usually leads to the presence of oscillations in the numerical results [7]. In [9] the authors described a first attempt to apply the Lagrange-projection strategy to a two-phase system, in particular the two-fluid two-pressure (or seven-equation) model. There, the coupling terms of the system have not been considered directly inside the Lagrange-projection decomposition but in a third step. In this work, we propose a different approach from the ones mentioned above.

Moreover, we also consider a different interpretation of the Lagrange-projection approach, namely the acoustic-transport splitting, refer again to the previous references. Indeed, by decomposing the different phenomena of the mathematical model, we obtain two different systems, the acoustic and transport one. For the former, we design an approximate Riemann solver based on a relaxation approach and then the associated Godunov-type scheme is used. We also explain how the resulting approximation can be exploited for the Lagrangian system. Furthermore, let us recall that the acoustic-transport splitting (or equivalently the Lagrange-projection decomposition) can be particularly interesting in subsonic regimes, where the acoustic waves are much faster than the transport ones. This means that an implicit approximation applied to the acoustic system could lead to the construction of very fast numerical schemes as we would neglect the acoustic time step condition. For this reason, we propose both an explicit and an implicit strategy for the acoustic equations, while keeping an explicit approximation for the transport step. For implicit-explicit Lagrange-projection methods refer for instance to [14, 15].

Last but not least, we are interested in the well-balanced property of the numerical schemes, meaning that the numerical methods are able to preserve the stationary solutions of the mathematical model, at least for the so-called lake-at-rest solutions. Indeed, it is well-known that otherwise we could observe spurious oscillations in the numerical simulations when near to a steady state, refer for instance to [8, 10, 11, 15, 17, 20] and to [2] for well-balanced schemes with and without the Lagrange-projection decomposition respectively. Therefore, let us see which are the stationary solutions of the model. They are generally given by the following relations

$$\begin{cases} h_j u_j = q_j^0 = \text{constant}, & \text{with } j = 1, 2 \\ \frac{q_1^0}{h_1^2} + g(h_1 + h_2 + z) = \text{constant} \\ \frac{q_2^0}{h_2^2} + g(rh_1 + h_2 + z) = \text{constant}. \end{cases} \quad (2)$$

Here we are particularly interested in preserving only the ones with zero velocity, usually known as lake-at-

rest solutions, namely

$$\begin{cases} u_j = 0, & \text{with } j = 1, 2 \\ h_1 = \text{constant} \\ h_2 + z = \text{constant}. \end{cases} \quad (3)$$

For fully well-balanced Lagrange-projection methods, refer to [8, 20].

Outline of the paper. To conclude this section, we give a brief outline of the manuscript. In Section 2 we formulate the mathematical model (1) in Lagrangian coordinates and we analyze a simplified version of it. In Section 3, the acoustic-transport decomposition is presented, leading to the description of an approximate Riemann solver for the acoustic system. Section 4 is devoted to the presentation of both the explicit and implicit-explicit numerical strategies. In particular, the well-balanced property is proved in both cases. Finally in Section 5 and 6 we respectively show numerical simulations and draw the conclusions.

2 Lagrangian coordinates

This section is devoted to the description of the mathematical model (1) in Lagrangian coordinates. After the introduction of an arbitrary fluid particle located at ξ , the usual procedure consists in describing the corresponding characteristic curves. Hence, due to the presence of two different velocities, one for each layer, it is convenient to define two different trajectories x_j such that

$$\begin{cases} \frac{\partial x_j}{\partial t}(\xi, t) = u_j(x_j(\xi, t), t) \\ x_j(\xi, 0) = \xi. \end{cases} \quad (4)$$

As a consequence, we define the volume ratio $L_j(\xi, t)$ for each layer, as in the following

$$L_j(\xi, t) = \frac{\partial x_j}{\partial \xi}(\xi, t) \quad \text{such that} \quad \begin{cases} \frac{\partial L_j}{\partial t}(\xi, t) = \partial_\xi u_j(x_j(\xi, t), t) \\ L_j(\xi, 0) = 1. \end{cases} \quad (5)$$

Then, any function $\varphi : (x_j, t) \rightarrow \varphi(x_j, t)$ (associated to the j th trajectory) in Eulerian coordinates can be expressed in Lagrangian coordinates,

$$\bar{\varphi}^{(j)}(\xi, t) = \varphi(x_j(\xi, t), t).$$

This means that we have to introduce new additional variables. Indeed, we generally need to distinguish between $\bar{\varphi}^{(1)}(\xi, t) = \varphi(x_1(\xi, t), t)$ and $\bar{\varphi}^{(2)}(\xi, t) = \varphi(x_2(\xi, t), t)$. Defining then the space and time derivatives,

$$\partial_\xi \bar{\varphi}^{(j)}(\xi, t) = L_j(\xi, t) \partial_x \varphi(x, t) \quad \text{and} \quad \partial_t \bar{\varphi}^{(j)}(\xi, t) = \partial_t \varphi(x, t) + u_j(x, t) \partial_x \varphi(x, t),$$

we are able to reformulate system (1) in Lagrangian coordinates as in the following,

$$\begin{cases} \partial_t(L_1 \bar{h}_1^{(1)}) = 0 \\ \partial_t(L_1 \bar{h}_1^{(1)} \bar{u}_1^{(1)}) + \partial_\xi \bar{p}_1^{(1)} + g \bar{h}_1^{(1)} L_1 \partial_x \bar{h}_2^{(1)} = -g \bar{h}_1^{(1)} \partial_\xi \bar{z}^{(1)} \\ \partial_t(L_2 \bar{h}_2^{(2)}) = 0 \\ \partial_t(L_2 \bar{h}_2^{(2)} \bar{u}_2^{(2)}) + \partial_\xi \bar{p}_2^{(2)} + g r \bar{h}_2^{(2)} L_2 \partial_x \bar{h}_1^{(2)} = -g \bar{h}_2^{(2)} \partial_\xi \bar{z}^{(2)}. \end{cases} \quad (6)$$

Observe that here we wrote the evolution equations for the variables $\bar{h}_1^{(1)}$, $\bar{h}_1^{(1)} \bar{u}_1^{(1)}$, $\bar{h}_2^{(2)}$ and $\bar{h}_2^{(2)} \bar{u}_2^{(2)}$ but four additional equations would be needed for the unknowns $\bar{h}_1^{(2)}$, $\bar{h}_1^{(2)} \bar{u}_1^{(2)}$, $\bar{h}_2^{(1)}$ and $\bar{h}_2^{(1)} \bar{u}_2^{(1)}$. However,

in the following we do an approximation in order to be able to neglect such variables. Indeed, after few manipulations and neglecting the superscript when it is equal to the subscript, we obtain

$$\begin{cases} \partial_t(L_1\bar{h}_1) = 0 \\ \partial_t(L_1\bar{h}_1\bar{u}_1) + \partial_\xi\bar{p}_1 + g\bar{h}_1\left(\frac{L_1}{L_2}\partial_\xi\bar{h}_2 + L_1\partial_x(\bar{h}_2^{(1)} - \bar{h}_2)\right) = -g\bar{h}_1\partial_\xi\bar{z}^{(1)} \\ \partial_t(L_2\bar{h}_2) = 0 \\ \partial_t(L_2\bar{h}_2\bar{u}_2) + \partial_\xi\bar{p}_2 + gr\bar{h}_2\left(\frac{L_2}{L_1}\partial_\xi\bar{h}_1 + L_2\partial_x(\bar{h}_1^{(2)} - \bar{h}_1)\right) = -g\bar{h}_2\partial_\xi\bar{z}^{(2)} \end{cases}$$

At this stage, we do an approximation and assume the terms $\partial_x(\bar{h}_2^{(1)} - \bar{h}_2)$ and $\partial_x(\bar{h}_1^{(2)} - \bar{h}_1)$ to be null as at initial time we have $\bar{h}_1|_{t=0} = \bar{h}_1^{(2)}|_{t=0} = h_1(x, t = 0)$ and $\bar{h}_2|_{t=0} = \bar{h}_2^{(1)}|_{t=0} = h_2(x, t = 0)$. From a numerical point of view, this implies that we are approximating these terms explicitly and at first-order of accuracy. Furthermore, we generally expect these two terms to be rather small when the velocities u_1 and u_2 are close. Hence, from now on we consider the following Lagrangian system

$$\begin{cases} \partial_t(L_1\bar{h}_1) = 0 \\ \partial_t(L_1\bar{h}_1\bar{u}_1) + \partial_\xi\bar{p}_1 + g\bar{h}_1\frac{L_1}{L_2}\partial_\xi\bar{h}_2 = -g\bar{h}_1\partial_\xi\bar{z}^{(1)} \\ \partial_t(L_2\bar{h}_2) = 0 \\ \partial_t(L_2\bar{h}_2\bar{u}_2) + \partial_\xi\bar{p}_2 + gr\bar{h}_2\frac{L_2}{L_1}\partial_\xi\bar{h}_1 = -g\bar{h}_2\partial_\xi\bar{z}^{(2)} \end{cases} \quad (7)$$

with pressures $p_j = g\frac{h_j^2}{2}$. It is clear that further studies are required in order to include the unknowns $\bar{h}_1^{(2)}$, $\bar{h}_1^{(2)}\bar{u}_1^{(2)}$, $\bar{h}_2^{(1)}$ and $\bar{h}_2^{(1)}\bar{u}_2^{(1)}$ in the system. More details about the Lagrange-projection decomposition applied to the shallow water system can be found for instance in [20].

Neglecting the bars over the unknowns, we reformulate equations (7) together with system (5) in a more compact way,

$$\partial_t\mathbf{LQ} + \mathbf{A}(\mathbf{LQ})\partial_\xi\mathbf{LQ} = \mathbf{S}(\mathbf{LQ}, z)$$

where

$$\mathbf{LQ} = \begin{pmatrix} L_1 \\ L_1\bar{h}_1 \\ L_1\bar{h}_1\bar{u}_1 \\ L_2 \\ L_2\bar{h}_2 \\ L_2\bar{h}_2\bar{u}_2 \end{pmatrix}, \quad \mathbf{A}(\mathbf{LQ}) = \begin{pmatrix} 0 & \frac{u_1}{L_1\bar{h}_1} & -\frac{1}{L_1\bar{h}_1} & 0 & 0 & 0 \\ 0 & 0 & 0 & 0 & 0 & 0 \\ -g\frac{h_1^2}{L_1} & g\frac{h_1}{L_1} & 0 & -g\frac{L_1\bar{h}_1\bar{h}_2}{L_2^2} & g\frac{L_1\bar{h}_1}{L_2^2} & 0 \\ 0 & 0 & 0 & 0 & \frac{u_2}{L_2\bar{h}_2} & -\frac{1}{L_2\bar{h}_2} \\ 0 & 0 & 0 & 0 & 0 & 0 \\ -gr\frac{L_2\bar{h}_2\bar{h}_1}{L_1^2} & gr\frac{L_2\bar{h}_2}{L_1^2} & 0 & -g\frac{h_2^2}{L_2} & g\frac{h_2}{L_2} & 0 \end{pmatrix}$$

and

$$\mathbf{S}(\mathbf{LQ}, z) = \begin{pmatrix} 0 \\ 0 \\ -g\bar{h}_1\partial_\xi\bar{z}^{(1)} \\ 0 \\ 0 \\ -g\bar{h}_2\partial_\xi\bar{z}^{(2)} \end{pmatrix}.$$

Moreover, observing that $L_j\bar{h}_j$ does not depend on time, we find

$$L_j\bar{h}_j(\xi, t) = L_j\bar{h}_j(\xi, 0) = h_j(\xi, 0) = h_j^0 \quad \text{and consequently} \quad L_j = \frac{h_j^0}{h_j},$$

and as such

$$\frac{L_1}{L_2} = \frac{h_1^0 \bar{h}_2}{h_2^0 \bar{h}_1}.$$

Thus, defining the variables $\tau_j = \frac{1}{h_j}$, we propose another formulation for system (7),

$$\begin{cases} \partial_t h_1^0 = 0 \\ \partial_t (h_1^0 \bar{\tau}_1) - \partial_\xi \bar{u}_1 = 0 \\ \partial_t (h_1^0 \bar{u}_1) + \partial_\xi \bar{p}_1 + \frac{h_1^0}{h_2^0} \partial_\xi \bar{p}_2 = -\frac{g}{\bar{\tau}_1} \partial_\xi \bar{z}^{(1)} \\ \partial_t h_2^0 = 0 \\ \partial_t (h_2^0 \bar{\tau}_2) - \partial_\xi \bar{u}_2 = 0 \\ \partial_t (h_2^0 \bar{u}_2) + \partial_\xi \bar{p}_2 + r \frac{h_2^0}{h_1^0} \partial_\xi \bar{p}_1 = -\frac{g}{\bar{\tau}_2} \partial_\xi \bar{z}^{(2)} \end{cases}$$

or equivalently,

$$\begin{cases} \partial_t \bar{\tau}_1 - \frac{1}{h_1^0} \partial_\xi \bar{u}_1 = 0 \\ \partial_t \bar{u}_1 + \frac{1}{h_1^0} \partial_\xi \bar{p}_1 + \frac{1}{h_2^0} \partial_\xi \bar{p}_2 = -\frac{g}{h_1^0 \bar{\tau}_1} \partial_\xi \bar{z}^{(1)} \\ \partial_t \bar{\tau}_2 - \frac{1}{h_2^0} \partial_\xi \bar{u}_2 = 0 \\ \partial_t \bar{u}_2 + \frac{1}{h_2^0} \partial_\xi \bar{p}_2 + \frac{r}{h_1^0} \partial_\xi \bar{p}_1 = -\frac{g}{h_2^0 \bar{\tau}_2} \partial_\xi \bar{z}^{(2)}. \end{cases} \quad (8)$$

The non-conservative matrix of the latter system reads

$$\begin{pmatrix} 0 & -\frac{1}{h_1^0} & 0 & 0 \\ \frac{1}{h_1^0} \partial_{\tau_1} p_1 & 0 & \frac{1}{h_2^0} \partial_{\tau_2} p_2 & 0 \\ 0 & 0 & 0 & -\frac{1}{h_2^0} \\ \frac{r}{h_1^0} \partial_{\tau_1} p_1 & 0 & \frac{1}{h_2^0} \partial_{\tau_2} p_2 & 0 \end{pmatrix},$$

whose characteristic polynomial is given by

$$\begin{aligned} & (\lambda^2 + \frac{\partial_{\tau_1} p_1}{h_{0,1}^2})(\lambda^2 + \frac{\partial_{\tau_2} p_2}{h_{0,2}^2}) - r \frac{\partial_{\tau_1} p_1}{h_{0,1}^2} \frac{\partial_{\tau_2} p_2}{h_{0,2}^2} = \\ & = \lambda^4 + (\frac{\partial_{\tau_1} p_1}{h_{0,1}^2} + \frac{\partial_{\tau_2} p_2}{h_{0,2}^2}) \lambda^2 + (1-r) \frac{\partial_{\tau_1} p_1 \partial_{\tau_2} p_2}{h_{0,1}^2 h_{0,2}^2} = \lambda^4 + (\alpha_1 + \alpha_2) \lambda^2 + (1-r) \alpha_1 \alpha_2 \end{aligned}$$

with $\alpha_1 = \frac{\partial_{\tau_1} p_1}{h_{0,1}^2} = -g \frac{h_1^3}{h_{0,1}^2}$, $\alpha_2 = \frac{\partial_{\tau_2} p_2}{h_{0,2}^2} = -g \frac{h_2^3}{h_{0,2}^2}$ and thus $\alpha_1, \alpha_2 \leq 0$. It is easy to see that the eigenvalues are then given by

$$\begin{aligned} \lambda_{ext}^\pm &= \pm \sqrt{\frac{-(\alpha_1 + \alpha_2) + \sqrt{(\alpha_1 + \alpha_2)^2 - 4(1-r)\alpha_1\alpha_2}}{2}}, \\ \lambda_{int}^\pm &= \pm \sqrt{\frac{-(\alpha_1 + \alpha_2) - \sqrt{(\alpha_1 + \alpha_2)^2 - 4(1-r)\alpha_1\alpha_2}}{2}} \end{aligned}$$

which can be proved to be always real. Indeed, we first observe that

$$(\alpha_1 + \alpha_2)^2 - 4(1-r)\alpha_1\alpha_2 = (\alpha_1 - \alpha_2)^2 + 4r\alpha_1\alpha_2 \geq 0,$$

from which it follows that λ_{ext}^\pm are real. Regarding λ_{int}^\pm , it is enough to note that

$$-(\alpha_1 + \alpha_2) - \sqrt{(\alpha_1 + \alpha_2)^2 - 4(1-r)\alpha_1\alpha_2} \geq 0$$

which holds true as $\alpha_1\alpha_2 \geq 0$. Thus it is interesting to remark that this simplified version of the Lagrangian system has always real eigenvalues.

Finally, let us underline that, in systems (7) and (8), we still have $\bar{z}^{(1)}$ and $\bar{z}^{(2)}$, which are generally different. However, since in section 4 we treat these topography source terms explicitly, once again we do an approximation and simply assume $\bar{z}^{(1)} = \bar{z}^{(2)} = z$.

3 Acoustic transport splitting

As it is already known, the Lagrange-projection splitting and the acoustic-transport one can be interpreted as two different ways of describing the same kind of decomposition. Indeed, it has already been illustrated the relation between the acoustic and Lagrangian numerical approximation, see for instance the following papers applied to the shallow water system [15], the gas dynamics equations [13] and the blood flow system [17]. Therefore, following the lines of these works, we present the acoustic-transport splitting for the two-layer shallow water model as it will be useful for the development of the numerical strategy. Hence, we decouple the different terms of the model obtaining the acoustic and transport system, respectively given by

$$\begin{cases} \partial_t h_1 + h_1 \partial_x u_1 = 0 \\ \partial_t (h_1 u_1) + h_1 u_1 \partial_x u_1 + \partial_x \frac{gh_1^2}{2} + gh_1 \partial_x h_2 = -gh_1 \partial_x z \\ \partial_t h_2 + h_2 \partial_x u_2 = 0 \\ \partial_t (h_2 u_2) + h_2 u_2 \partial_x u_2 + \partial_x \frac{gh_2^2}{2} + grh_2 \partial_x h_1 = -gh_2 \partial_x z \end{cases} \quad (9)$$

and

$$\begin{cases} \partial_t h_1 + u_1 \partial_x h_1 = 0 \\ \partial_t (h_1 u_1) + u_1 \partial_x h_1 u_1 = 0 \\ \partial_t h_2 + u_2 \partial_x h_2 = 0 \\ \partial_t (h_2 u_2) + u_2 \partial_x h_2 u_2 = 0. \end{cases} \quad (10)$$

We also observe that the latter simply reads as $\partial_t X_j + u_j \partial_x X_j = 0$ with $X = h, hu$ and $j = 1, 2$. On the other hand, after few computations, system (9) can be reformulated as

$$\begin{cases} \partial_t h_1 + h_1 \partial_x u_1 = 0 \\ \partial_t u_1 + \frac{1}{h_1} \partial_x \frac{gh_1^2}{2} + g \partial_x h_2 = -g \partial_x z \\ \partial_t h_2 + h_2 \partial_x u_2 = 0 \\ \partial_t u_2 + \frac{1}{h_2} \partial_x \frac{gh_2^2}{2} + gr \partial_x h_1 = -g \partial_x z \end{cases}$$

and again

$$\begin{cases} \partial_t \tau_1 - \tau_1 \partial_x u_1 = 0 \\ \partial_t u_1 + \tau_1 \partial_x \frac{g}{2\tau_1^2} + \tau_2 \partial_x \frac{g}{2\tau_2^2} = -g \partial_x z \\ \partial_t \tau_2 - \tau_2 \partial_x u_2 = 0 \\ \partial_t u_2 + r\tau_1 \partial_x \frac{g}{2\tau_1^2} + \tau_2 \partial_x \frac{g}{2\tau_2^2} = -g \partial_x z. \end{cases} \quad (11)$$

where we have introduced the variables $\tau_j = \frac{1}{h_j}$, $j = 1, 2$. It is then evident the similarity between the Lagrangian system (8) and the acoustic equations (11).

A first difficulty is related to the fact that usually the mass variable m is introduced for the acoustic system at this stage, see for instance the previous references [15, 13, 17]. For example, in the shallow water system, this new variable m is defined such that $\partial_m = \frac{1}{h} \partial_x$ with h the water height. Subsequently, it allows to obtain a conservation form of the equations (at least when there is no source term), making easier the definition of the numerical strategy. However, having in this case two different water heights h_1 and h_2 , it is not clear how to include such a device and thus, here we do not consider it.

Since we do not know the general exact solution of a Riemann Problem (RP) associated to the acoustic system (11), we look for an approximate Riemann solver. In order to be able to define it, it is convenient to start applying a linearization of the non-linear terms present in the equations. Therefore, considering the following form for the acoustic system

$$\begin{cases} \partial_t \tau_1 - \tau_1 \partial_x u_1 = 0 \\ \partial_t u_1 + \partial_x \frac{g}{\tau_1} + \partial_x \frac{g}{\tau_2} = -g \partial_x z \\ \partial_t \tau_2 - \tau_2 \partial_x u_2 = 0 \\ \partial_t u_2 + r \partial_x \frac{g}{\tau_1} + \partial_x \frac{g}{\tau_2} = -g \partial_x z, \end{cases} \quad (12)$$

we introduce the relaxation parameter λ and two new variables $\mathcal{C}_1, \mathcal{C}_2$ such that they satisfy

$$\lim_{\lambda \rightarrow \infty} \mathcal{C}_1 = g \frac{1}{\tau_1} = gh_1 \quad \text{and} \quad \lim_{\lambda \rightarrow \infty} \mathcal{C}_2 = g \frac{1}{\tau_2} = gh_2 \quad (13)$$

at least formally. Hence, we are able to define the following relaxation system

$$\begin{cases} \partial_t \tau_1 - \tau_1 \partial_x u_1 = 0 \\ \partial_t u_1 + \partial_x \mathcal{C}_1 + \partial_x \mathcal{C}_2 = -g \partial_x z \\ \partial_t \tau_2 - \tau_2 \partial_x u_2 = 0 \\ \partial_t u_2 + r \partial_x \mathcal{C}_1 + \partial_x \mathcal{C}_2 = -g \partial_x z. \\ \partial_t \mathcal{C}_1 + a_1^2 \partial_x u_1 = \frac{1}{\lambda} \left(g \frac{1}{\tau_1} - \mathcal{C}_1 \right) \\ \partial_t \mathcal{C}_2 + a_2^2 \partial_x u_2 = \frac{1}{\lambda} \left(g \frac{1}{\tau_2} - \mathcal{C}_2 \right). \end{cases} \quad (14)$$

where a_1, a_2 are constant parameters.

Proposition 1. *The relaxation system (14) is stable under the sub-characteristic condition $a_j^2 \geq c_j^2 = gh_j$.*

Proof. To prove it, we start writing the following first-order correction for \mathcal{C}_j ,

$$\mathcal{C}_j = g \frac{1}{\tau_j} + \lambda \mathcal{C}_j^{(1)} + \mathcal{O}(\lambda^2), \quad (15)$$

which we insert into the evolution equations for \mathcal{C}_j , obtaining

$$-\mathcal{C}_j^{(1)} + \mathcal{O}(\lambda) = g \partial_t \frac{1}{\tau_j} + a_j^2 \partial_x u_j = -g \frac{1}{\tau_j^2} \partial_t \tau_j + a_j^2 \partial_x u_j = \left(-g \frac{1}{\tau_j} + a_j^2 \right) \partial_x u_j. \quad (16)$$

Afterwards, neglecting the source term, we consider relations (16) together with equations (14) which lead to the following system

$$\partial_t \mathbf{W} + \mathbf{E}(\mathbf{W}) \partial_x \mathbf{W} = \lambda \partial_x (\mathbf{D}(\mathbf{W}) \partial_x \mathbf{W}) + \mathcal{O}(\lambda^2)$$

with $\mathbf{W} = (\tau_1, u_1, \tau_2, u_2)^T$ and

$$\mathbf{D}(\mathbf{W}) = \begin{pmatrix} 0 & 0 & 0 & 0 \\ 0 & -g\frac{1}{\tau_1} + a_1^2 & 0 & -g\frac{1}{\tau_2} + a_2^2 \\ 0 & 0 & 0 & 0 \\ 0 & r(-g\frac{1}{\tau_1} + a_1^2) & 0 & -g\frac{1}{\tau_2} + a_2^2 \end{pmatrix}.$$

Finally, we need to impose that $\mathbf{D}(\mathbf{W})$ is a diffusion matrix, namely that its eigenvalues are non-negative. From this condition, we obtain the following sub-characteristic conditions $a_j^2 \geq gh_j$. \square

Moreover, since we assume \mathcal{C}_j to be well-prepared in the sense that $\mathcal{C}_j(x, t = 0) = gh_j(x, t = 0)$, we neglect the source terms $\frac{1}{\lambda}(g\frac{1}{\tau_j} - \mathcal{C}_j)$ in the evolution equations for \mathcal{C}_j . Then, we rewrite system (14) in a more compact form as

$$\partial_t \mathbf{U} + \mathbf{A}(\mathbf{U})\partial_x \mathbf{U} = \tilde{\mathbf{S}}(\mathbf{U}, z)$$

where $\mathbf{U} = (\tau_1, u_1, \tau_2, u_2, \mathcal{C}_1, \mathcal{C}_2)^T$,

$$\mathbf{A}(\mathbf{U}) = \begin{pmatrix} 0 & -\tau_1 & 0 & 0 & 0 & 0 \\ 0 & 0 & 0 & 0 & 1 & 1 \\ 0 & 0 & 0 & -\tau_2 & 0 & 0 \\ 0 & 0 & 0 & 0 & r & 1 \\ 0 & a_1^2 & 0 & 0 & 0 & 0 \\ 0 & 0 & 0 & a_2^2 & 0 & 0 \end{pmatrix} \quad \text{and} \quad \tilde{\mathbf{S}}(\mathbf{U}, z) = \begin{pmatrix} 0 \\ -g\partial_x z \\ 0 \\ 0 \\ -g\partial_x z \end{pmatrix}.$$

and then we find its characteristic polynomial

$$\lambda^4(\lambda^4 - (a_1^2 + a_2^2)\lambda^2 + (1 - r)a_1^2 a_2^2).$$

Its roots are given by $\lambda_0 = 0$,

$$\lambda_{ext}^{\pm} = \pm \sqrt{\frac{a_1^2 + a_2^2 + \sqrt{(a_1^2 + a_2^2)^2 - 4(1 - r)a_1^2 a_2^2}}{2}} \quad (17)$$

and

$$\lambda_{int}^{\pm} = \pm \sqrt{\frac{a_1^2 + a_2^2 - \sqrt{(a_1^2 + a_2^2)^2 - 4(1 - r)a_1^2 a_2^2}}{2}},$$

where once again it can be easily proved that the eigenvalues are always real since we assume the water heights to be positive. Moreover, it is also clear that the eigenvalues are ordered a priori, namely

$$\lambda_{ext}^- < \lambda_{int}^- < \lambda_0 = 0 < \lambda_{int}^+ < \lambda_{ext}^+.$$

Subsequently, we look for the right eigenvectors of form

$$\mathbf{R} = (r_1, r_2, r_3, r_4, r_5, r_6)^t.$$

Then, associated to the zero eigenvalue λ_0 we easily obtain

$$\mathbf{R}_1^{\lambda_0} = \begin{pmatrix} 1 \\ 0 \\ 0 \\ 0 \\ 0 \\ 0 \end{pmatrix}, \quad \mathbf{R}_2^{\lambda_0} = \begin{pmatrix} 0 \\ 0 \\ 1 \\ 0 \\ 0 \\ 0 \end{pmatrix},$$

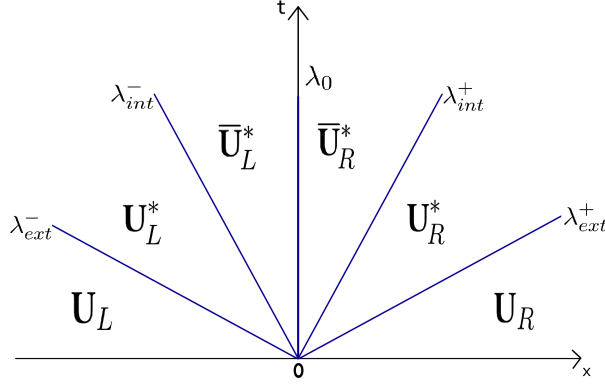


Figure 2: Sketch of the approximate solution for the Riemann problem.

otherwise we have

$$\mathbf{R}^\lambda = \begin{pmatrix} 1 \\ \lambda \\ -\frac{\lambda}{\tau_1} \\ \beta \\ -\frac{\lambda}{\tau_2} \\ \beta \\ -\frac{a_1^2}{\tau_1} \\ -\frac{a_2^2}{\tau_2} \\ \beta \end{pmatrix}$$

where $\beta = \frac{\tau_2 a_1^2}{\tau_1 a_2^2} \left(\frac{\lambda^2}{a_1^2} - 1 \right)$. Finally, few computations give us the Riemann invariants. Across the zero-discontinuity we get

$$\text{RI}_{u_j}^{\lambda_0} = u_j, \quad \text{RI}_{C_j}^{\lambda_0} = C_j,$$

while for the other waves with speed $\lambda \neq 0$,

$$\text{RI}_{1,j}^\lambda = C_j - \frac{a_j^2}{\lambda} u_j, \quad \text{RI}_{2,j}^\lambda = C_j + a_j^2 \ln \tau_j, \quad \text{RI}_3^\lambda = C_2 + \left(1 - \frac{\lambda^2}{a_1^2} \right) C_1.$$

3.1 Approximate Riemann solver for the acoustic system

Here we look for the approximate solution of the Riemann problem associated to system (14) with the following initial conditions

$$\mathbf{U}(x, t = 0) = \begin{cases} \mathbf{U}_L & \text{if } x < 0 \\ \mathbf{U}_R & \text{if } x > 0 \end{cases} \quad (18)$$

where

$$\mathbf{U}_L = \begin{pmatrix} \tau_{1,L} \\ u_{1,L} \\ \tau_{2,L} \\ u_{2,L} \\ C_{1,L} \\ C_{2,L} \end{pmatrix} \quad \text{and} \quad \mathbf{U}_R = \begin{pmatrix} \tau_{1,R} \\ u_{1,R} \\ \tau_{2,R} \\ u_{2,R} \\ C_{1,R} \\ C_{2,R} \end{pmatrix}.$$

Since we have five discontinuities, the solution of the Riemann problem consists of six separated states, namely

$$\mathbf{U}\left(\frac{x}{t}; \mathbf{U}_L, \mathbf{U}_R\right) = \begin{cases} \mathbf{U}_L & \text{if } \frac{x}{t} < \lambda_{ext}^- \\ \mathbf{U}_L^* & \text{if } \lambda_{ext}^- < \frac{x}{t} < \lambda_{int}^- \\ \bar{\mathbf{U}}_L^* & \text{if } \lambda_{int}^- < \frac{x}{t} < \lambda_0 \\ \bar{\mathbf{U}}_R^* & \text{if } \lambda_0 < \frac{x}{t} < \lambda_{int}^+ \\ \mathbf{U}_R^* & \text{if } \lambda_{int}^+ < \frac{x}{t} < \lambda_{ext}^+ \\ \mathbf{U}_R & \text{if } \frac{x}{t} > \lambda_{ext}^+ \end{cases} \quad (19)$$

where in particular

$$\mathbf{U}_L^* = \begin{pmatrix} \tau_{1,L}^* \\ u_{1,L}^* \\ \tau_{2,L}^* \\ u_{2,L}^* \\ \mathcal{C}_{1,L}^* \\ \mathcal{C}_{2,L}^* \end{pmatrix} \quad \bar{\mathbf{U}}_L^* = \begin{pmatrix} \bar{\tau}_{1,L}^* \\ \bar{u}_{1,L}^* \\ \bar{\tau}_{2,L}^* \\ \bar{u}_{2,L}^* \\ \bar{\mathcal{C}}_{1,L}^* \\ \bar{\mathcal{C}}_{2,L}^* \end{pmatrix} \quad \mathbf{U}_R^* = \begin{pmatrix} \tau_{1,R}^* \\ u_{1,R}^* \\ \tau_{2,R}^* \\ u_{2,R}^* \\ \mathcal{C}_{1,R}^* \\ \mathcal{C}_{2,R}^* \end{pmatrix} \quad \bar{\mathbf{U}}_R^* = \begin{pmatrix} \bar{\tau}_{1,R}^* \\ \bar{u}_{1,R}^* \\ \bar{\tau}_{2,R}^* \\ \bar{u}_{2,R}^* \\ \bar{\mathcal{C}}_{1,R}^* \\ \bar{\mathcal{C}}_{2,R}^* \end{pmatrix}, \quad (20)$$

refer also to Figure (2). Due to the fact that a_j are constant, it is clear that characteristic fields associated to the eigenvalues are linearly degenerate and thus that all the waves are contact discontinuities. Therefore, in order to find the Riemann solution, we can exploit the Riemann invariants or equivalently the Rankine-Hugoniot jump conditions.

We underline that the star values for u_j and \mathcal{C}_j can be found without exploiting the ones for τ_j . Therefore, for the sake of conciseness and since in the numerical strategies we only need the star values for u_j and \mathcal{C}_j , here we do not include the definitions for the star values for τ_j but they can be found in an analogous way.

Starting with the jump conditions across the zero-discontinuity and including the topography in the solver, we impose

$$\begin{cases} \bar{u}_{j,L}^* = \bar{u}_{j,R}^* = \bar{u}_j^* & \text{with } j = 1, 2 \\ \bar{\mathcal{C}}_{1,R}^* - \bar{\mathcal{C}}_{1,L}^* + \bar{\mathcal{C}}_{2,R}^* - \bar{\mathcal{C}}_{2,L}^* + \mathcal{M} = 0 \\ r(\bar{\mathcal{C}}_{1,R}^* - \bar{\mathcal{C}}_{1,L}^*) + \bar{\mathcal{C}}_{2,R}^* - \bar{\mathcal{C}}_{2,L}^* + \mathcal{M} = 0 \end{cases}$$

where $\mathcal{M} = \Delta x \{g \partial_x z\}$ is a function that has to be defined but it should be zero when $z_L = z_R$. Thus, we simply ask for

$$\mathcal{M} = g(z_R - z_L).$$

As far as the other waves are concerned, from the Riemann invariants presented in the previous section, we get the following conditions associated to λ_{ext}^-

$$\begin{cases} \mathcal{C}_{j,L} - \frac{a_j^2}{\lambda_{ext}^-} u_{j,L} = \mathcal{C}_{j,L}^* - \frac{a_j^2}{\lambda_{ext}^-} u_{j,L}^* & \text{with } j = 1, 2 \\ \mathcal{C}_{2,L}^* + \left(1 - \frac{(\lambda_{ext}^-)^2}{a_1^2}\right) \mathcal{C}_{1,L}^* = \mathcal{C}_{2,L} + \left(1 - \frac{(\lambda_{ext}^-)^2}{a_1^2}\right) \mathcal{C}_{1,L}, \end{cases}$$

associated to λ_{int}^-

$$\begin{cases} \mathcal{C}_{j,L}^* - \frac{a_j^2}{\lambda_{int}^-} u_{j,L}^* = \bar{\mathcal{C}}_{j,L}^* - \frac{a_j^2}{\lambda_{int}^-} \bar{u}_j^* & \text{with } j = 1, 2 \\ \mathcal{C}_{2,L}^* + \left(1 - \frac{(\lambda_{int}^-)^2}{a_1^2}\right) \mathcal{C}_{1,L}^* = \bar{\mathcal{C}}_{2,L}^* + \left(1 - \frac{(\lambda_{int}^-)^2}{a_1^2}\right) \bar{\mathcal{C}}_{1,L}^*, \end{cases}$$

associated to λ_{int}^+

$$\begin{cases} \mathcal{C}_{j,R}^* - \frac{a_j^2}{\lambda_{int}^+} u_{j,R}^* = \bar{\mathcal{C}}_{j,R}^* - \frac{a_j^2}{\lambda_{int}^+} \bar{u}_j^* & \text{with } j = 1, 2 \\ \mathcal{C}_{2,R}^* + (1 - \frac{(\lambda_{int}^+)^2}{a_1^2}) \mathcal{C}_{1,R}^* = \bar{\mathcal{C}}_{2,R}^* + (1 - \frac{(\lambda_{int}^+)^2}{a_1^2}) \bar{\mathcal{C}}_1^*, \end{cases}$$

and finally associated to λ_{ext}^+

$$\begin{cases} \mathcal{C}_{j,R}^* - \frac{a_j^2}{\lambda_{ext}^+} u_{j,R}^* = \mathcal{C}_{j,R} - \frac{a_j^2}{\lambda_{ext}^+} u_{j,R} & \text{with } j = 1, 2 \\ \mathcal{C}_{2,R}^* + (1 - \frac{(\lambda_{ext}^+)^2}{a_1^2}) \mathcal{C}_{1,R}^* = \mathcal{C}_{2,R} + (1 - \frac{(\lambda_{ext}^+)^2}{a_1^2}) \mathcal{C}_{1,R}. \end{cases}$$

Since we had 16 unknowns and we found 16 relations, we are able to solve the resulting system. Thus, after some computations, we can explicitly write the star states as in the following,

$$\begin{cases} \mathcal{C}_{1,R}^* = \mathcal{C}_{1,R} - \frac{a_1^2 - (\lambda_{int}^+)^2}{2((\lambda_{ext}^+)^2 - (\lambda_{int}^+)^2)} (\mathcal{C}_{1,R} - \mathcal{C}_{1,L}) - \frac{a_1^2}{2((\lambda_{ext}^+)^2 - (\lambda_{int}^+)^2)} (\mathcal{C}_{2,R} - \mathcal{C}_{2,L} + \mathcal{M} + \mathcal{U}) \\ \mathcal{C}_{1,L}^* = \mathcal{C}_{1,L} + \frac{a_1^2 - (\lambda_{int}^+)^2}{2((\lambda_{ext}^+)^2 - (\lambda_{int}^+)^2)} (\mathcal{C}_{1,R} - \mathcal{C}_{1,L}) + \frac{a_1^2}{2((\lambda_{ext}^+)^2 - (\lambda_{int}^+)^2)} (\mathcal{C}_{2,R} - \mathcal{C}_{2,L} + \mathcal{M} - \mathcal{U}) \\ \bar{\mathcal{C}}_1^* = \frac{\mathcal{C}_{1,R} + \mathcal{C}_{1,L}}{2} - \frac{a_1^2}{2\lambda_{int}^+} (u_{1,R} - u_{1,L}) + \frac{a_1^2}{2\lambda_{int}^+} \frac{\mathcal{U}}{\lambda_{ext}^+ + \lambda_{int}^+} \\ \mathcal{C}_{2,R}^* = \mathcal{C}_{2,R} + \frac{a_1^2 - (\lambda_{ext}^+)^2}{2a_1^2((\lambda_{ext}^+)^2 - (\lambda_{int}^+)^2)} \left((a_1^2 - (\lambda_{int}^+)^2) (\mathcal{C}_{1,R} - \mathcal{C}_{1,L}) + a_1^2 (\mathcal{C}_{2,R} - \mathcal{C}_{2,L} + \mathcal{M} + \mathcal{U}) \right) \\ \mathcal{C}_{2,L}^* = \mathcal{C}_{2,L} - \frac{a_1^2 - (\lambda_{ext}^+)^2}{2a_1^2((\lambda_{ext}^+)^2 - (\lambda_{int}^+)^2)} \left((a_1^2 - (\lambda_{int}^+)^2) (\mathcal{C}_{1,R} - \mathcal{C}_{1,L}) + a_1^2 (\mathcal{C}_{2,R} - \mathcal{C}_{2,L} + \mathcal{M} - \mathcal{U}) \right) \\ \bar{\mathcal{C}}_2^* = \frac{\mathcal{C}_{2,R} + \mathcal{C}_{2,L}}{2} - \frac{a_2^2}{2\lambda_{int}^+} (u_{2,R} - u_{2,L}) - \frac{1}{2\lambda_{int}^+} \frac{(a_1^2 - (\lambda_{ext}^+)^2) \mathcal{U}}{\lambda_{ext}^+ + \lambda_{int}^+} \\ \bar{\mathcal{C}}_{2,R}^* = \bar{\mathcal{C}}_2^* - \frac{\mathcal{M}}{2} \\ \bar{\mathcal{C}}_{2,L}^* = \bar{\mathcal{C}}_2^* + \frac{\mathcal{M}}{2} \\ u_{1,R}^* = u_{1,R} - \frac{\lambda_{ext}^+}{2((\lambda_{ext}^+)^2 - (\lambda_{int}^+)^2)} (\mathcal{K}_2^+ + \mathcal{M} + (1 - \frac{(\lambda_{int}^+)^2}{a_1^2}) \mathcal{K}_1^+) \\ u_{1,L}^* = u_{1,L} - \frac{\lambda_{ext}^+}{2((\lambda_{ext}^+)^2 - (\lambda_{int}^+)^2)} (\mathcal{K}_2^- + \mathcal{M} + (1 - \frac{(\lambda_{int}^+)^2}{a_1^2}) \mathcal{K}_1^-) \\ \bar{u}_1^* = \frac{u_{1,R} + u_{1,L}}{2} - \frac{\lambda_{int}^+}{2a_1^2} (\mathcal{C}_{1,R} - \mathcal{C}_{1,L}) - \frac{\mathcal{P} + \mathcal{M}}{2(\lambda_{ext}^+ + \lambda_{int}^+)} \\ u_{2,R}^* = u_{2,R} + \frac{\lambda_{ext}^+}{2((\lambda_{ext}^+)^2 - (\lambda_{int}^+)^2)} \frac{a_1^2 - (\lambda_{ext}^+)^2}{a_2^2} (\mathcal{K}_2^+ + \mathcal{M} + (1 - \frac{(\lambda_{int}^+)^2}{a_1^2}) \mathcal{K}_1^+) \\ u_{2,L}^* = u_{2,L} + \frac{\lambda_{ext}^+}{2((\lambda_{ext}^+)^2 - (\lambda_{int}^+)^2)} \frac{a_1^2 - (\lambda_{ext}^+)^2}{a_2^2} (\mathcal{K}_2^- + \mathcal{M} + (1 - \frac{(\lambda_{int}^+)^2}{a_1^2}) \mathcal{K}_1^-) \\ \bar{u}_2^* = \frac{u_{2,R} + u_{2,L}}{2} - \frac{\lambda_{int}^+}{2a_2^2} (\mathcal{C}_{2,R} - \mathcal{C}_{2,L} + \mathcal{M}) + \frac{a_1^2}{a_2^2} (1 - \frac{(\lambda_{ext}^+)^2}{a_1^2}) \frac{\mathcal{P} + \mathcal{M}}{2(\lambda_{ext}^+ + \lambda_{int}^+)} \end{cases} \quad (21)$$

where the following quantities were introduced to lighten the formulas

$$\mathcal{U} = \frac{a_2^2}{\lambda_{ext}^+} (u_{2,R} - u_{2,L}) + \frac{a_1^2 - (\lambda_{int}^+)^2}{\lambda_{ext}^+} (u_{1,R} - u_{1,L}), \quad \mathcal{P} = \mathcal{C}_{2,R} - \mathcal{C}_{2,L} + (1 - \frac{(\lambda_{int}^+)^2}{a_1^2}) (\mathcal{C}_{1,R} - \mathcal{C}_{1,L}),$$

and

$$\mathcal{K}_j^\pm = \mathcal{C}_{j,R} - \mathcal{C}_{j,L} \pm \frac{a_j^2}{\lambda_{ext}^+} (u_{j,R} - u_{j,L}).$$

4 Numerical approximation

Before describing the numerical scheme, it is necessary to give some details about the space and time discretizations. We start defining the constant space step Δx and the time step Δt . Then, the mesh interfaces are given by $x_{i+1/2} = i\Delta x$ for $i \in \mathbb{Z}$ and the intermediate times by $t^n = n\Delta t$ for $n \in \mathbb{N}$. As far as the variable ξ is concerned, we use the same space discretization of x , hence $\Delta\xi = \Delta x$, $\xi_{i+1/2} = x_{i+1/2}$ and $\xi_i = x_i \forall i$.

Concerning the numerical strategy, since we have two different steps (Lagrangian and projection) or systems (acoustic and transport), the numerical method is composed of two stages as well:

1. Update \mathbf{Q}^n to \mathbf{Q}^{n+1-} by solving the acoustic or Lagrangian system;
2. Exploit \mathbf{Q}^{n+1-} to solve either the transport system or the projection step and find \mathbf{Q}^{n+1} .

Finally, we underline that we present both an explicit and implicit approximation of the first step. Clearly, depending on which formulation we use, also the Courant–Friedrichs–Lewy (CFL) condition [22] on the time step changes. Indeed, in general for the acoustic step we ask for the following

$$\Delta t \leq \frac{\Delta x}{2} \frac{1}{\max_i \{\lambda_{ext,i+1/2}^+\}} \quad (22)$$

with λ_{ext}^+ given by (17), while in the case of the transport stage we impose

$$\Delta t \leq \frac{\Delta x}{2} \frac{1}{\max_i \{(\bar{u}_{j,i-1/2}^*)^+ - (\bar{u}_{j,i+1/2}^*)^-\}} \quad \text{for } j = 1, 2 \quad (23)$$

with $(\bar{u}_{j,i-1/2}^*)^+ = \max(\bar{u}_{j,i-1/2}^*, 0)$ and $(\bar{u}_{j,i+1/2}^*)^- = \min(\bar{u}_{j,i+1/2}^*, 0)$. Then, the final time step should be taken as the minimum between the two. However, if we use an implicit approximation for the Lagrangian step we could neglect condition (22) and exploit only the transport one (23).

4.1 Explicit approximation of the acoustic-Lagrangian system

Considering the Godunov method associated to the approximate Riemann solver of the previous section 3.1, the updating formula is given by

$$\begin{aligned} \mathbf{U}_i^{n+1-} = & \mathbf{U}_i^n - \frac{\Delta t}{\Delta x} \left(\lambda_{ext,i-1/2}^{+,n} (\mathbf{U}_i^n - \mathbf{U}_{R,i-1/2}^*) + \lambda_{int,i-1/2}^{+,n} (\mathbf{U}_{R,i-1/2}^* - \bar{\mathbf{U}}_{R,i-1/2}^*) + \right. \\ & \left. + \lambda_{ext,i+1/2}^{+,n} (\mathbf{U}_i^n - \mathbf{U}_{L,i+1/2}^*) + \lambda_{int,i+1/2}^{+,n} (\mathbf{U}_{L,i+1/2}^* - \bar{\mathbf{U}}_{L,i+1/2}^*) \right) \end{aligned} \quad (24)$$

which is simply given by a juxtaposition of the approximate solutions of the Riemann problems defined locally at each interface, refer for instance to [22].

As far as the acoustic system is concerned, to update the variables h_j , hu_j , we could use the Godunov method, namely (24). In practice, since we would like to use the Lagrangian variables, we do the following. We indeed find u_j^{n+1-} using formula (24), then for the water heights we simply exploit

$$Lh_{j,i}^{n+1-} = Lh_{j,i}^n = h_{j,i}^n$$

and finally we state

$$Lh_{j,i}^{n+1-} u_{j,i}^{n+1-} = Lh_{j,i}^n u_{j,i}^{n+1-} = h_{j,i}^n u_{j,i}^{n+1-}.$$

Thus, we do not actually use the Godunov updating formula for the evolution equations for τ_j^{n+1-} , namely $\partial_t \tau_j - \tau_j \partial_x u_j = 0$, but only for the equations for the velocities, which are written in conservative form.

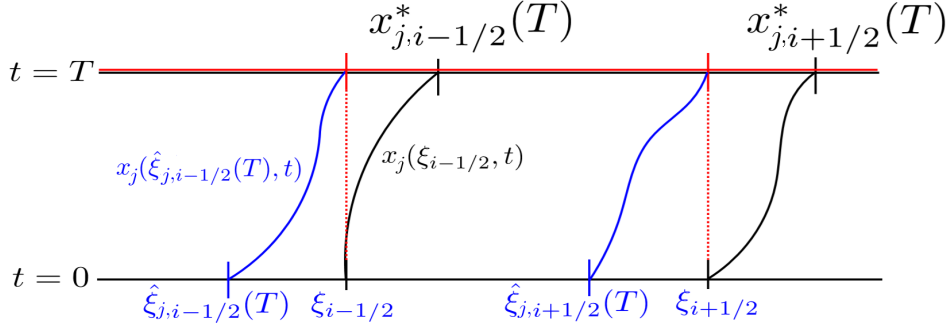


Figure 3: Sketch of the connection between Lagrangian and Eulerian coordinates.

4.3 Transport-projection step

Let us finally see how to discretize the transport system or projection step. The two approximations will be very similar, still different.

Regarding the former, since we have two sets of two equations of form $\partial_t X_j + u_j \partial_x X_j = 0$ with $X = h, hu$ and $j = 1, 2$, we observe that

$$\partial_t X_j + u_j \partial_x X_j = \partial_t X_j - X_j \partial_x u_j + \partial_x (X u)_j = 0,$$

thus we simply exploit the following explicit approximation

$$X_{j,i}^{n+1} = X_{j,i}^{n+1-} \left(1 + \frac{\Delta t}{\Delta x} (\bar{u}_{j,i+1/2}^* - \bar{u}_{j,i-1/2}^*) \right) - \frac{\Delta t}{\Delta x} (\bar{u}_{j,i+1/2}^* X_{j,i+1/2}^{n+1-} - \bar{u}_{j,i-1/2}^* X_{j,i-1/2}^{n+1-}).$$

In particular, the latter discretization is equivalent to

$$X_{j,i}^{n+1} = (LX)_{j,i}^{n+1-} - \frac{\Delta t}{\Delta x} (\bar{u}_{j,i+1/2}^* X_{j,i+1/2}^{n+1-} - \bar{u}_{j,i-1/2}^* X_{j,i-1/2}^{n+1-}) \quad (31)$$

where we used an explicit upwind discretization for $X_{j,i+1/2}^{n+1-}$, namely

$$X_{j,i+1/2}^{n+1-} = \begin{cases} X_{j,i}^{n+1-} & \text{if } \bar{u}_{j,i+1/2}^* \geq 0 \\ X_{j,i+1}^{n+1-} & \text{if } \bar{u}_{j,i+1/2}^* < 0. \end{cases}$$

Next, let us move on to the projection step discretization. In order to be able to explain it, it is convenient to give few details about the link between Eulerian and Lagrangian coordinates, for which we also refer to Figure 3. Recall that we use the index j for the layer and i for the cell of the mesh, we define $\hat{\xi}_{j,i+1/2}(t)$ such that $\forall i$

$$x_j(\hat{\xi}_{j,i+1/2}(T), T) = x_{i+1/2}, \quad \text{with } T \geq 0,$$

where the corresponding trajectories are given by

$$\begin{cases} \frac{\partial x_j}{\partial t}(\hat{\xi}_{j,i+1/2}(T), t) = u_j(x_j(\hat{\xi}_{j,i+1/2}(T), t), t) \\ x_j(\hat{\xi}_{j,i+1/2}(T), 0) = \hat{\xi}_{j,i+1/2}(T). \end{cases}$$

Therefore, it is easy to obtain the following approximation $x_{i+1/2} = \hat{\xi}_{j,i+1/2} + \Delta t u_{j,i+1/2}^*$. Similarly, we also find $x_{j,i+1/2}^{*,n+1-} = x_{i+1/2} + \Delta t u_{j,i+1/2}^*$ and thus $x_{i+1/2} - x_{j,i+1/2}^* = \hat{\xi}_{j,i+1/2} - \xi_{i+1/2}$. Moving to the integrals of the variables, we can change coordinates as in the following

$$\int_{x_j(\xi_{j,l}, t)}^{x_j(\xi_{j,r}, t)} X_j(x, t) dx = \int_{\xi_{j,l}}^{\xi_{j,r}} L_j(\xi, t) \bar{X}_j(\xi, t) d\xi.$$

leading to

$$X_{j,i}(t) = \frac{1}{\Delta x} \int_{x_{i-\frac{1}{2}}}^{x_{i+\frac{1}{2}}} X_j(x, t) dx = \frac{1}{\Delta x} \int_{x_j(\hat{\xi}_{j,i-\frac{1}{2}}, t)}^{x_j(\hat{\xi}_{j,i+\frac{1}{2}}, t)} X_j(x, t) dx = \frac{1}{\Delta x} \int_{\hat{\xi}_{j,i-\frac{1}{2}}}^{\hat{\xi}_{j,i+\frac{1}{2}}} L_j(\xi, t) \bar{X}_j(\xi, t) d\xi. \quad (32)$$

Therefore, splitting the integrals in three parts

$$\begin{aligned} X_{j,i}^{n+1} &= \frac{1}{\Delta x} \int_{\hat{\xi}_{j,i-\frac{1}{2}}}^{\xi_{i-\frac{1}{2}}} L_j(\xi, t^{n+1-}) \bar{X}_j(\xi, t^{n+1-}) d\xi + \\ &+ \frac{1}{\Delta x} \int_{\xi_{i-\frac{1}{2}}}^{\xi_{i+\frac{1}{2}}} L_j(\xi, t^{n+1-}) \bar{X}_j(\xi, t^{n+1-}) d\xi + \frac{1}{\Delta x} \int_{\xi_{i+\frac{1}{2}}}^{\hat{\xi}_{j,i+\frac{1}{2}}} L_j(\xi, t^{n+1-}) \bar{X}_j(\xi, t^{n+1-}) d\xi. \end{aligned} \quad (33)$$

and approximating them, we obtain

$$X_{j,i}^{n+1} = (LX)_{j,i}^{n+1-} - \frac{\Delta t}{\Delta x} (\bar{u}_{j,i+1/2}^* (LX)_{j,i+1/2}^{n+1-} - \bar{u}_{j,i-1/2}^* (LX)_{j,i-1/2}^{n+1-}) \quad (34)$$

where

$$(LX)_{j,i+1/2}^{n+1-} = \begin{cases} (LX)_{j,i}^{n+1-} & \text{if } \bar{u}_{j,i+1/2}^* \geq 0 \\ (LX)_{j,i+1}^{n+1-} & \text{if } \bar{u}_{j,i+1/2}^* < 0 \end{cases}$$

$\forall i$. For similar procedure applied to the shallow water system or the blood flow equations, see respectively [20] and [17]. Hence, the only difference between formulation (31) and (34) is related to the use of the variable X or LX in the definition of the numerical fluxes. Observe that, in the numerical simulations, we always use formulation (34).

4.4 Properties of the numerical scheme

Considering the explicit and implicit Lagrangian approximations (26),(30) and the projection formulation (34), we can find an overall approximation for the two-layer shallow water system (1),

$$\left\{ \begin{aligned} h_{1,i}^{n+1} &= h_{1,i}^n - \frac{\Delta t}{\Delta x} (\bar{u}_{1,i+1/2}^{*,\#} (Lh)_{1,i+1/2}^{n+1-} - \bar{u}_{1,i-1/2}^{*,\#} (Lh)_{1,i-1/2}^{n+1-}) \\ (hu)_{1,i}^{n+1} &= (hu)_{1,i}^n - h_{1,i}^n \frac{\Delta t}{\Delta x} (\bar{c}_{1,i+1/2}^{*,\#} - \bar{c}_{1,i-1/2}^{*,\#} + \bar{c}_{2,i+1/2}^{*,\#} - \bar{c}_{2,i-1/2}^{*,\#}) + \\ &\quad - \frac{\Delta t}{\Delta x} (\bar{u}_{1,i+1/2}^{*,\#} (Lh)_{1,i+1/2}^{n+1-} - \bar{u}_{1,i-1/2}^{*,\#} (Lh)_{1,i-1/2}^{n+1-}) + h_{1,i}^n \Delta t \frac{S_{i+1/2} + S_{i-1/2}}{2} \\ h_{2,i}^{n+1} &= h_{2,i}^n - \frac{\Delta t}{\Delta x} (\bar{u}_{2,i+1/2}^{*,\#} (Lh)_{2,i+1/2}^{n+1-} - \bar{u}_{2,i-1/2}^{*,\#} (Lh)_{2,i-1/2}^{n+1-}) \\ (hu)_{2,i}^{n+1} &= (hu)_{2,i}^n - h_{2,i}^n \frac{\Delta t}{\Delta x} (r(\bar{c}_{1,i+1/2}^{*,\#} - \bar{c}_{1,i-1/2}^{*,\#}) + \bar{c}_{2,i+1/2}^{*,\#} - \bar{c}_{2,i-1/2}^{*,\#}) \cdot \\ &\quad - \frac{\Delta t}{\Delta x} (\bar{u}_{2,i+1/2}^{*,\#} (Lh)_{2,i+1/2}^{n+1-} - \bar{u}_{2,i-1/2}^{*,\#} (Lh)_{2,i-1/2}^{n+1-}) + h_{2,i}^n \Delta t \frac{S_{i+1/2} + S_{i-1/2}}{2}. \end{aligned} \right. \quad (35)$$

with either $\# = n$ or $\# = n + 1 -$ depending on the explicit and implicit approximation.

Remark 1. The numerical approximation (35) preserves the positivity of the water heights h_1, h_2 . Indeed, it is enough to exploit the CFL condition (23) to prove it.

Theorem 1. The numerical approximation (35) with star values (21) is well-balanced in the sense it preserves the stationary solution (3).

Proof. We start assuming that the stationary solution (3) is satisfied at time t^n , namely $u_{j,i}^n = 0$, $h_{1,i}^n = h_{1,i+1}^n$ and $h_{2,i}^n + z_i = h_{2,i+1}^n + z_{i+1} \forall i$, we want to prove that $h_{j,i}^{n+1} = h_{j,i}^n$ and $(hu)_{j,i}^{n+1} = (hu)_{j,i}^n$ for $j = 1, 2$ and $\forall i$.

Then, first of all we consider the explicit approximation. Since $\mathcal{C}_{2,i+1} - \mathcal{C}_{2,i} + \mathcal{M} = g(h_{2,i+1} - h_{2,i} + z_{i+1} - z_i) = 0$ and $u_{j,i} = 0$ by hypothesis, it is straightforward to see that $\bar{u}_{1,i-1/2}^{*,n} = \bar{u}_{2,i-1/2}^{*,n} = 0$. Similarly we get $\mathcal{C}_{1,i+1/2}^{*,n} = \mathcal{C}_{1,i}$ and $\mathcal{C}_{2,i+1/2}^{*,n} = \frac{\mathcal{C}_{2,i} + \mathcal{C}_{2,i+1}}{2}$. Observing that $\mathcal{C}_{2,i+1/2}^{*,n} - \mathcal{C}_{2,i-1/2}^{*,n} = \frac{S_{i+1/2} + S_{i-1/2}}{2}$, we get $h_{j,i}^{n+1} = h_{j,i}^{n+1-} = h_{j,i}^n$ and $(hu)_{j,i}^{n+1} = (hu)_{j,i}^{n+1-} = (hu)_{j,i}^n$ for $j = 1, 2$ and $\forall i$. Thus, we proved that the explicit approximation is well-balanced. Let us now move to the implicit one. The heart of the proof is to show that, when we are under the lake at rest condition, system (28) can be reformulated in a form as $AU^{n+1-} = AU^n$ with A matrix which would lead to the conclusion of the proof. Indeed, it is easy to see such a thing as $u_{j,i}^n = 0 \forall i$, for $j = 1, 2$ while for the water heights we have $h_{1,i}^n = h_{1,i+1}^n$ and $h_{2,i+1}^n - h_{2,i}^n = -z_{i+1} + z_i \forall i$. \square

5 Numerical simulations

In the following, we are interested in comparing the numerical results of the four following numerical schemes:

- "IFCP" (Intermediate Field Capturing Parabola) method applied to the two-layer shallow water system (1), for which we refer to [18];
- "LP-ARS" scheme, for which we use the explicit acoustic approximation described in section 4.1 and the transport discretization (34);
- "LP-ARS-IMP" method, for which we use the implicit acoustic approximation described in section 4.2 and the transport discretization (34);
- "LP-HLL" scheme, where once again we use the transport discretization (34) but we approximate the Lagrangian step by applying the HLL strategy to the Lagrangian system (7), see for instance [22] or appendix B.

Observe that the IFCP solutions are taken as a reference to establish if the proposed numerical strategies can be considered satisfying.

Furthermore, we use $r = 0.98$ and transmissive boundary conditions. As far as the LP-ARS-IMP method is concerned, we consider both the acoustic (22) and transport (23) CFL conditions with $CFL = 0.5$ unless otherwise stated. Finally, we underline that for all the numerical simulations, we exploited MATLAB language with a single Intel Core i7 CPU.

5.1 Riemann problems

Using $M = 200$ cells, we start considering academic test cases, namely two Riemann problems.

RP 1. Taking into account a channel of length $L = 10$ m, we consider a dam-break problem for the interface. More explicitly, we take the following initial data, $u_1(x, t = 0) = 0$, $u_2(x, t = 0) = 0$ and

$$h_{1,L} = 0.2, \quad h_{1,R} = 0.8, \quad h_{2,L} = 0.8, \quad h_{2,R} = 0.2,$$

refer also to [18] for more details about this and the following Riemann problem.

In Figure 4 we show the results for the water heights h_1 , h_2 and fluxes q_1 , q_2 using the four above-mentioned methods. In general, we observe that all the schemes give analogous solutions where in particular the IFCP and LP-HLL methods are respectively the less and the most diffusive. It is not surprising the difference

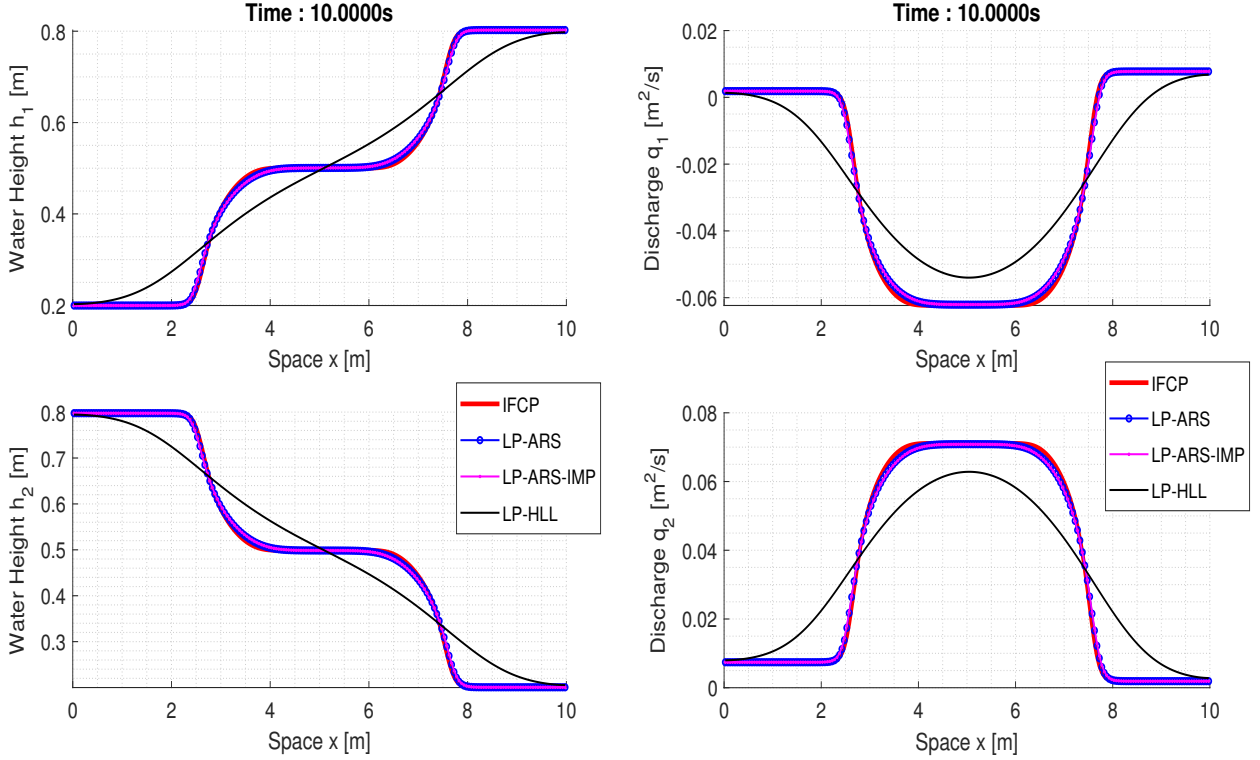


Figure 4: RP 1 of section 5.1: water height h_1, h_2 (left) and discharge q_1, q_2 (right). IFCP (red), LP-ARS (blue), LP-ARS-IMP (magenta) and LP-HLL (black) outputs obtained with $M = 200$ cells at time $t = 10$ s.

in accuracy between the IFCP and the LP-HLL as the HLL strategy neglects the internal waves. Nevertheless, refining the mesh, we observed that the LP-HLL solution seems to converge towards the reference output. On the other hand, it is important to underline that the LP-ARS method gives results very close to the IFCP ones. Moreover, since we have used the same time step, the LP-ARS-IMP outputs are only slightly more diffusive than the LP-ARS ones. Let us conclude observing that we could have used a much larger time step for the implicit method as we are in a sub-critical regime. For this reason, we now consider a series of meshes ($M = 64, 128, 256, 512$ cells) in order to compare the efficiency of the two methods. Thus, for the implicit LP-ARS-IMP method we only use the transport CFL condition (23) and neglect the acoustic one (22). Then, we compute the reference solution with the IFCP method and $M = 2048$ cells. Finally, in table 1 we insert the errors in norm \mathbf{L}^1 while in table 2 we show the computational times. As expected the errors of the LP-ARS-IMP scheme are slightly greater than those of the LP-ARS method. On the other hand, we immediately see that the LP-ARS-IMP scheme allows faster simulations.

| Mesh | Error (\mathbf{L}^1) of h_1 | | Error (\mathbf{L}^1) of q_1 | | Error (\mathbf{L}^1) of h_2 | | Error (\mathbf{L}^1) of q_2 | |
|------|-----------------------------------|------------|-----------------------------------|------------|-----------------------------------|------------|-----------------------------------|------------|
| | LP-ARS | LP-ARS-IMP | LP-ARS | LP-ARS-IMP | LP-ARS | LP-ARS-IMP | LP-ARS | LP-ARS-IMP |
| 64 | 0.2630 | 0.3063 | 0.0561 | 0.0661 | 0.2604 | 0.3038 | 0.0556 | 0.0657 |
| 128 | 0.1714 | 0.2169 | 0.0367 | 0.0467 | 0.1697 | 0.2143 | 0.0364 | 0.0458 |
| 256 | 0.1059 | 0.1440 | 0.0230 | 0.0312 | 0.1048 | 0.1429 | 0.0227 | 0.0311 |
| 512 | 0.0605 | 0.0900 | 0.0134 | 0.0204 | 0.0598 | 0.0891 | 0.0132 | 0.0202 |

Table 1: Errors in norm \mathbf{L}^1 of the variables $h_j, q_j = h_j u_j$ with $j = 1, 2$ using LP-ARS and LP-ARS-IMP schemes. Meshes of size $M = (64, 128, 256, 512)$ cells.

RP 2. As a second test, we consider a channel of length $L = 100$ with discontinuity in the middle. The

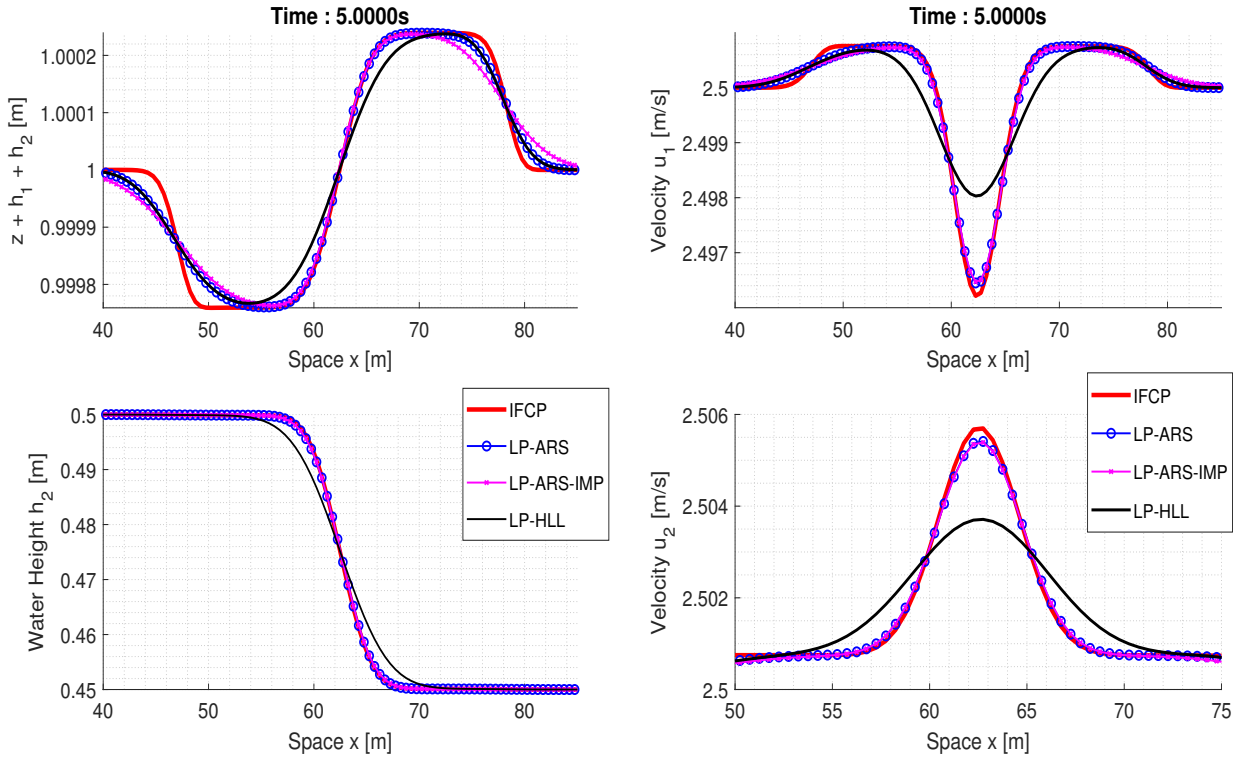


Figure 5: RP 2 of section 5.1: free surface $h_1 + h_2$, water height h_2 (left) and velocity u_1, u_2 (right). IFCP (red), LP-ARS (blue), LP-ARS-IMP (magenta) and LP-HLL (black) outputs obtained with $M = 200$ cells at time $t = 5$ s.

| Method | $M = 64$ | $M = 128$ | $M = 256$ | $M = 512$ |
|------------|----------|-----------|-----------|-----------|
| LP-ARS | 0.213301 | 0.588727 | 1.907348 | 6.749875 |
| LP-ARS-IMP | 0.0319 | 0.1070 | 0.5477 | 3.4986 |

Table 2: Computational times in seconds for LP-ARS and LP-ARS-IMP schemes with meshes of size $M = (64, 128, 256, 512)$ cells.

initial conditions for the water heights are given by

$$h_{1,L} = 0.5, \quad h_{1,R} = 0.55, \quad h_{2,L} = 0.5, \quad h_{2,R} = 0.45,$$

while for the fluxes we state

$$q_{1,L} = 1.25, \quad q_{1,R} = 1.375, \quad q_{2,L} = 1.25, \quad q_{2,R} = 1.125,$$

see again [18]. Then, Figure 5 shows the different outputs which generally confirms what we have observed for the previous Riemann problem. The solutions are in agreement with the ones presented in [18].

5.2 Stationary solution and perturbation

Next, we numerically verify that our numerical strategy is indeed well-balanced in the sense that it preserves the stationary solution (3). Thus, we take $L = 1$ and as initial condition we consider the following steady state

$$h_1(x, t = 0) = 1, \quad h_2(x, t = 0) + z(x) = 1, \quad u_1(x, t = 0) = 0, \quad u_2(x, t = 0) = 0, \quad (36)$$

where

$$z(x) = \begin{cases} \frac{1}{4}(1 + \cos(\pi \frac{x-0.5}{0.1})) & \text{if } 0.4 \leq x \leq 0.6 \\ 0 & \text{otherwise.} \end{cases}$$

Our numerical methods are indeed able to preserve this stationary solution up to a machine error of order 10^{-13} computed in the \mathbf{L}^∞ norm using $t = 5$ s as ending time and the initial condition as exact solution.

Let us now introduce a small perturbation of the steady state, namely

$$h_1(x, t = 0) = \begin{cases} 1 + 10^{-5} & \text{if } 0.1 \leq x \leq 0.2 \\ 1 & \text{otherwise.} \end{cases}$$

In Figure 6 we show the LP-ARS results at different times and we observe that the perturbations propagate away so that we are able to recover the zero-velocity steady state (36). Indeed, the outputs are in agreement with the ones presented in [3]. We did not include the solutions for the other schemes as they are analogous. However, it is interesting to observe that LP-HLL solution is almost identical to the LP-ARS one while the LP-ARS-IMP output is more diffusive even if we use the same CFL condition.

5.3 Transcritical non-smooth stationary solution

In this section we aim to verify that our schemes are able to recover a transcritical non-smooth stationary solution if proper steady boundary conditions are imposed. We refer the reader to [5] for further details on this simulation. As a second step, we will also introduce some perturbations in the resulting steady state.

Thus, let us consider a channel of length $L = 10$ m and the following initial conditions

$$(hu)_j(x, t = 0) = 0, \quad h_1(x, t = 0) = \begin{cases} 0.5 & \text{if } x < 5 \\ 0.001 & \text{otherwise,} \end{cases}$$

$z(x) = 1 + 0.5x^{-(x-5)^2}$ and finally $h_2(x, t = 0) = 2 - (h_1(x, t = 0) + z(x))$. Then, for the boundary conditions we impose $(hu)_2 = -(hu)_1$ on both sides and $h_1(x = L, t) + h_2(x = L, t) + z(x = L) = 2$ at the end of the channel. In Figure 7 we include the results and compare the different outputs found at time $t = 1000$ s. Referring to [18], the flow is sub-critical for $x \geq 5$ while for $x < 5$ is supercritical at the beginning and then it becomes sub-critical as well. Thus, it is clear that at $x = 5$ there is a critical flow. First of all, we generally observe that all the numerical schemes are able to recover the aimed non-smooth

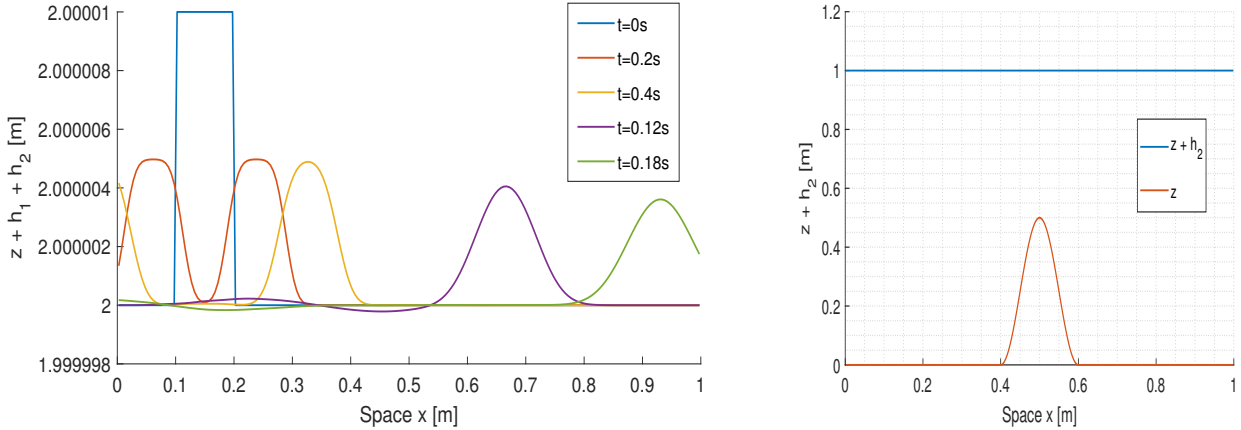


Figure 6: Evolution of the perturbation in the lake at rest steady state, section 5.2. LP-ARS solution for the free surface $h_1 + h_2 + z$ (left) for different times: $t = 0$ (blue), $t = 0.02$ (red), $t = 0.04$ (yellow), $t = 0.12$ (violet), $t = 0.18$ (green), $t = 0.26$ (light blue line). on the right, LP-ARS solution for $h_2 + z$ (blue) and topography z (red). $M = 200$ cells.

| Method | $M = 44$ | $M = 88$ | $M = 175$ | $M = 350$ |
|------------|----------|-----------|------------|------------|
| LP-ARS | 8.103190 | 25.550884 | 100.167893 | 363.242909 |
| LP-ARS-IMP | 1.666153 | 4.393538 | 34.577729 | 219.775353 |

Table 3: Computational times in seconds for LP-ARS and LP-ARS-IMP schemes with meshes of size $M = (44, 88, 175, 350)$ cells.

stationary solution even if some differences in the shock position and the left state value are present for the same mesh value $M = 350$ cells. However, in the IFCP results, some spurious oscillations are observed during the simulation. This is indeed natural since the internal eigenvalues can become complex in a small area of the supercritical region. On the other hand, unphysical oscillations are not observed when using the LP-ARS and LP-ARS-IMP schemes, probably partly related to the fact that the eigenvalues of the acoustic system are always real. Moreover, also the LP-HLL gives a solution without spurious oscillations. However, this is not surprising as the method neglect the middle waves of the mathematical model. Indeed, we can observe that the LP-HLL output is much more diffusive than the others.

Finally, since we are in a sub-critical regime, for the implicit scheme we could use a larger time step. On the right hand side in Figure 7, we show the LP-ARS-IMP solution computed taking as time step the minimum between the transport time step and the acoustic time step, where the latter is computed using as CFL values $\text{CFL} = 0.5, 2.5, 5$. Thus, once again, the solutions seem correct with some differences in the left state value. Then, in table 3, for different mesh values, we also include the computational times of the LP-ARS and LP-ARS-IMP schemes, where for the latter we use $\text{CFL} = 5$ for the acoustic time step condition. Once again, we generally see that the LP-ARS-IMP method is faster even if the regime is not always sub-critical. Moreover, it is clear that, the more we refine the mesh, the smaller will be the difference of the computational times between the two schemes.

5.3.1 Perturbation of the transcritical non-smooth stationary solution

Next, we consider the transcritical non-smooth stationary solution obtained in Section 5.3 as initial condition and we add a perturbation in the interface. The objective is to verify that the perturbation propagates

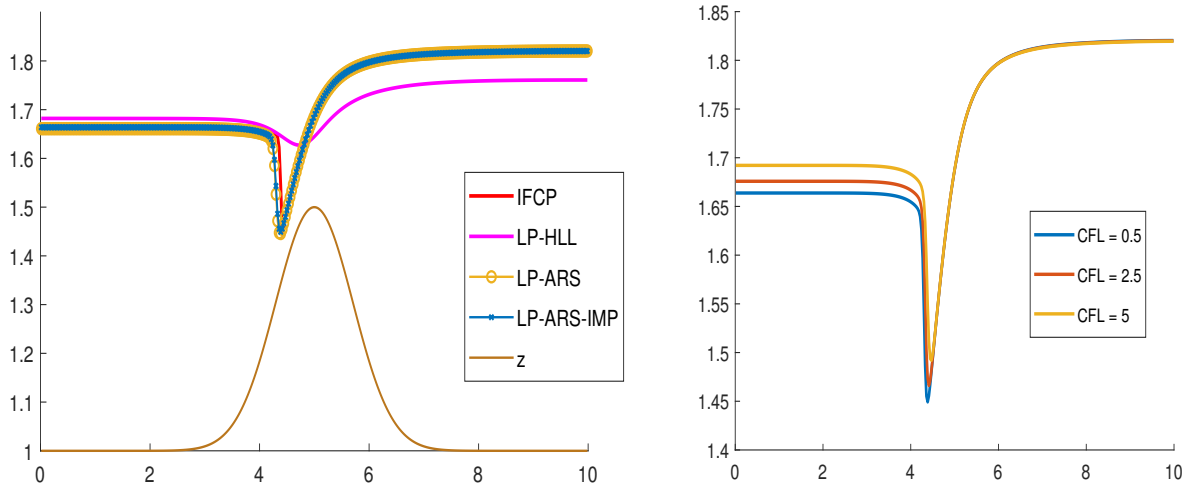


Figure 7: Transcritical non smooth stationary solution, section 5.3. On the left: IFCP (red), LP-HLL (magenta), LP-ARS (yellow) and LP-ARS-IMP (blue) solution for the interface $h_2 + z$. On the right: LP-ARS-IMP solution for $h_2 + z$ computed with $CFL = 0.5$ (blue), $CFL = 2.5$ (red) and $CFL = 5$ (yellow). $M = 350$ cells.

away and we recover the non-smooth stationary solution. Thus, at initial time we impose

$$h_2(x, t = 0) = \begin{cases} h_2^{eq} + 0.1e^{-100(x-6.5)^2} & \text{if } 6 \leq x \leq 7, \\ h_{eq} & \text{otherwise} \end{cases}$$

where the superscript "eq" indicates the transcritical non-smooth steady state. Regarding the boundary conditions, we keep the same as before. Results are shown in Figure 8 using the LP-ARS-IMP scheme. We do not include the results for the other methods as they are analogous. Indeed, we observe the perturbation propagates away at different times $t = 0, 0.15, 0.5, 1s$.

6 Concluding remarks

In this work the classic Lagrange-Projection (LP) approach has been extended to a two-velocities case, namely the two-layer shallow water system. Hence, we started this work presenting the mathematical model formulated in Lagrangian coordinates. To numerically approximate such a system, we also considered the acoustic-transport splitting, an alternative interpretation to the Lagrange-Projection decomposition. In particular, we were able to build an approximate Riemann solver for the acoustic system and to develop the associated Godunov-type scheme, both explicitly and implicitly. We underline that such a discretization can also be interpreted as an approximation for the Lagrangian system. Moreover, in the implicit version of the scheme, to find the numerical solution we only need to solve a linear system, which entails a not excessive computational cost. In this way, we were able to obtain a fast implicit-explicit method as we could use very large time steps, especially in sub-critical regimes.

Numerical simulations were proposed, in which we compared our results against the outputs of the well-known IFCP scheme. We also considered a LP-HLL method, meaning that the HLL approach has been applied to the simplified Lagrangian system (7), while keeping the same numerical strategy for the projection step. In the numerical tests, the LP-ARS strategy (both explicit and implicit) gave satisfying results, generally slightly more diffusive than the IFCP ones but much more accurate than the LP-HLL outputs.

Furthermore, it is interesting to underline that in the LP strategy we considered an approximated version of the Lagrangian system, obtaining in this way a new model for which we are able to explicitly write the eigenvalues and to prove that they are always real. Therefore, the numerical method is able to advance in

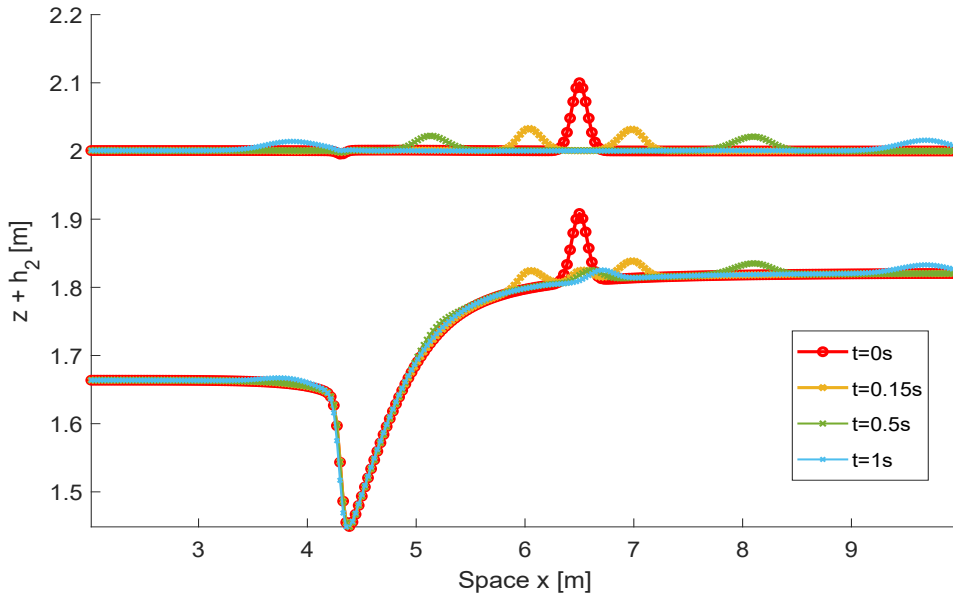


Figure 8: Evolution of the perturbation of a transcritical non smooth stationary solution, section 5.3.1. LP-ARS-IMP solution for the free surface $h_1 + h_2 + z$ and interface $h_2 + z$ for different times: $t = 0$ s (red), $t = 0.15$ s (yellow), $t = 0.5$ s (green) and $t = 1$ s (blue). $M = 350$ cells.

time even if there are small non-hyperbolic regions with complex internal eigenvalues. Indeed, in the test of Section 5.3, we acknowledged that our schemes do not produce spurious oscillations, contrarily to the IFCP method.

Acknowledgments

A. Del Grosso research has been supported by a grant from Région Île-de-France. M.J Castro research has been partially supported by the Spanish Government and FEDER through the coordinated Research project RTI2018-096064-B-C1, the Junta de Andalucía research project P18-RT-3163, the Junta de Andalucía-FEDER-University of Málaga research project UMA18-FEDERJA-16 and the University of Málaga. Tomás Morales de Luna has been partially supported by the Spanish Government and FEDER through the coordinated Research project RTI2018-096064-B-C2.

References

- [1] Rémi Abgrall and Smadar Karni. Two-Layer Shallow Water System: A Relaxation Approach. *SIAM J. Scientific Computing*. 31: 1603-1627, 2009. 10.1137/06067167X.
- [2] E. Audusse, F. Bouchut, M.O. Bristeau, R. Kleinc and B. Perthame. A fast and stable well-balanced scheme with hydrostatic reconstruction for shallow water flows. *SIAM Journal on Scientific Computing*, 25: 2050-2065, 2004. 10.1137/S1064827503431090.
- [3] J. Balbás and S. Karni. A Non-oscillatory Central Scheme for One-Dimensional Two-Layer Shallow Water Flows along Channels with Varying Width. *Journal of Scientific Computing*. 55: 499-528, 2013. 10.1007/s10915-012-9642-3.

- [4] F. Bouchut and T. Morales de Luna. An entropy satisfying scheme for two-layer shallow water equations with uncoupled treatment. *ESAIM: Mathematical Modelling and Numerical Analysis (ESAIM: M2AN)*, 42: 683–698, 2008. 10.1051/m2an:2008019
- [5] M. Castro, E. Fernández-Nieto, J. González Vida, C. Madroñal. Numerical Treatment of the Loss of Hyperbolicity of the Two-Layer Shallow-Water System. *Journal of Scientific Computing*. 48: 16-40, 2011. 10.1007/s10915-010-9427-5.
- [6] M. Castro, T. Morales de Luna, C. Madroñal. Well-Balanced Schemes and Path-Conservative Numerical Methods. 18: 131-175, 2016. 10.1016/bs.hna.2016.10.002.
- [7] M. J. Castro Díaz, Jorge Macías and Carlos Parés. A Q-scheme for a class of systems of coupled conservation laws with source term. Application to a two-layer 1-D shallow water system. *ESAIM M2AN Math. Model. Numer. Anal.* 35: 107–127, 2001. 10.1051/m2an:2001108
- [8] M. Castro, C. Chalons, T. Morales de Luna. A Fully Well-Balanced Lagrange–Projection-Type Scheme for the Shallow-Water Equations. *SIAM Journal on Numerical Analysis*. 56: 3071-3098, 2018. 10.1137/17M1156101.
- [9] C. Chalons, F. Coquel, S. Kokh, N. Spillane. Large time-step numerical scheme for the seven-equation model of compressible two-phase flows. *Springer Proceedings in Mathematics, FVCA 6*, 4(1): 225-233, 2011. 10.1007/978-3-642-20671-9_24
- [10] C. Chalons, A. Del Grosso. A second-order well-balanced Lagrange-projection scheme for Shallow Water Exner equations in 1D and 2D. 2021. (hal-03251707)
- [11] C. Chalons, A. Del Grosso. Exploring different possibilities for second-order well-balanced Lagrange-projection numerical schemes applied to shallow water Exner equations. *International Journal for Numerical Methods in Fluids*. 1- 31, 2022. 10.1002/fld.5064
- [12] C. Chalons, M. Girardin, S. Kokh. An all-regime Lagrange-Projection like scheme for 2D homogeneous models for two-phase flows on unstructured meshes. *Journal of Computational Physics, Elsevier*, 335: 885-904, 2017. 10.1016/j.jcp.2017.01.017.
- [13] C. Chalons, M. Girardin, S. Kokh. An All-Regime Lagrange-Projection Like Scheme for the Gas Dynamics Equations on Unstructured Meshes. *Communications in Computational Physics*. 20(1): 188-233 2016. 10.4208/cicp.260614.061115a.
- [14] C. Chalons, M. Girardin, S. Kokh. Large Time Step and Asymptotic Preserving Numerical Schemes for the Gas Dynamics Equations with Source Terms. *SIAM Journal on Scientific Computing*. 35(6):A2874–A2902, 2013. 10.1137/130908671.
- [15] C. Chalons, P. Kestener, S. Kokh, and M. Stauffert. A large time-step and well-balanced Lagrange-Projection type scheme for the Shallow-water equations. *Communications in Mathematical Sciences*. 15(3):765–788, 2017. 10.4310/CMS.2017.v15.n3.a9.
- [16] G. Dal Maso, P. G. Lefloch, and F. Murat. Definition and weak stability of nonconservative products. *Journal de Mathématiques Pures et Appliquées*, 74(6): 483–548, 1995.
- [17] A. Del Grosso and C. Chalons. Second-order well balanced Lagrange-Projection schemes for Blood Flow Equations. *Calcolo* 58, 43, 2021. 10.1007/s10092-021-00434-5
- [18] E. Fernández-Nieto, M. Castro, C. Parés. On an Intermediate Field Capturing Riemann Solver Based on a Parabolic Viscosity Matrix for the Two-Layer Shallow Water System. *Journal of Scientific Computing*. 48: 117-140, 2011. 10.1007/s10915-011-9465-7.

- [19] J. Lin, B. Mao, X. Lu. A Two-Layer Hydrostatic-Reconstruction Method for High-Resolution Solving of the Two-Layer Shallow-Water Equations over Uneven Bed Topography. *Mathematical Problems in Engineering*, 1-14, 2019. 10.1155/2019/5064171.
- [20] T. Morales De Luna, M. J. Castro Díaz and C. Chalons. High order fully well-balanced Lagrange-Projection scheme for Shallow-water. *Commun. Math. Sci.*, 18(3): 781–807, 2020. 10.4310/CMS.2020.v18.n3.a9
- [21] J.B. Schijf, J.C. Schonfeld. Theoretical considerations on the motion of salt and fresh water. In: *Proc. of the Minn. Int. Hydraulics Conv.*, 321–333. Joint meeting IAHR and Hyd. Div. ASCE, Sept. 1953.
- [22] E. F. Toro. *Riemann Solvers and Numerical Methods for Fluid Dynamics*, Third Edition. Springer–Verlag, 2009.

A Linear system for the implicit acoustic approximation

Considering the implicit approximation for the acoustic system presented in section 4.2, here we simply aim to show the form of the matrix A present in the linear system (29). In particular, we have a square matrix with $4M \times 4M$ entries where only 12 of them could be not null in each line, indeed

$$A = \begin{bmatrix} d_i^{u1} & d_i^{u2} & d_i^{C1} & d_i^{C2} & f_i^{u1} & f_i^{u2} & f_i^{C1} & f_i^{C2} & 0 & \dots & \dots & \dots & \dots & \dots & \dots & 0 \\ k_i^{u1} & k_i^{u2} & k_i^{C1} & k_i^{C2} & l_i^{u1} & l_i^{u2} & l_i^{C1} & l_i^{C2} & 0 & \dots & \dots & \dots & \dots & \dots & \dots & \vdots \\ n_i^{u1} & n_i^{u2} & n_i^{C1} & n_i^{C2} & q_i^{u1} & q_i^{u2} & q_i^{C1} & q_i^{C2} & 0 & \dots & \dots & \dots & \dots & \dots & \dots & \vdots \\ v_i^{u1} & v_i^{u2} & v_i^{C1} & v_i^{C2} & w_i^{u1} & w_i^{u2} & w_i^{C1} & w_i^{C2} & 0 & \dots & \dots & \dots & \dots & \dots & \dots & \vdots \\ \dots & \dots & \dots & \dots & \dots & \dots & \dots & \dots & \dots & \dots & \dots & \dots & \dots & \dots & \dots & \vdots \\ \dots & \dots & \dots & \dots & \dots & \dots & \dots & \dots & \dots & \dots & 0 & \dots & \dots & \dots & \dots & \vdots \\ \dots & \dots & \dots & \dots & \dots & \dots & \dots & \dots & \dots & \dots & 0 & \dots & \dots & \dots & \dots & \vdots \\ \dots & \dots & \dots & \dots & \dots & \dots & \dots & \dots & \dots & \dots & 0 & \dots & \dots & \dots & \dots & \vdots \\ \dots & \dots & \dots & \dots & \dots & \dots & \dots & \dots & \dots & \dots & 0 & \dots & \dots & \dots & \dots & \vdots \\ \dots & 0 & b_i^{u1} & b_i^{u2} & b_i^{C1} & b_i^{C2} & d_i^{u1} & d_i^{u2} & d_i^{C1} & d_i^{C2} & f_i^{u1} & f_i^{u2} & f_i^{C1} & f_i^{C2} & 0 & \dots \\ \dots & 0 & g_i^{u1} & g_i^{u2} & g_i^{C1} & g_i^{C2} & k_i^{u1} & k_i^{u2} & k_i^{C1} & k_i^{C2} & l_i^{u1} & l_i^{u2} & l_i^{C1} & l_i^{C2} & 0 & \dots \\ \dots & 0 & m_i^{u1} & m_i^{u2} & m_i^{C1} & m_i^{C2} & n_i^{u1} & n_i^{u2} & n_i^{C1} & n_i^{C2} & q_i^{u1} & q_i^{u2} & q_i^{C1} & q_i^{C2} & 0 & \dots \\ \dots & 0 & s_i^{u1} & s_i^{u2} & s_i^{C1} & s_i^{C2} & v_i^{u1} & v_i^{u2} & v_i^{C1} & v_i^{C2} & w_i^{u1} & w_i^{u2} & w_i^{C1} & w_i^{C2} & 0 & \dots \\ \dots & \dots & \dots & \dots & \dots & 0 & \dots & \dots & \dots & \dots & \dots & \dots & \dots & \dots & \dots & \vdots \\ \dots & \dots & \dots & \dots & \dots & 0 & \dots & \dots & \dots & \dots & \dots & \dots & \dots & \dots & \dots & \vdots \\ \dots & \dots & \dots & \dots & \dots & 0 & \dots & \dots & \dots & \dots & \dots & \dots & \dots & \dots & \dots & \vdots \\ \dots & \dots & \dots & \dots & \dots & 0 & \dots & \dots & \dots & \dots & \dots & \dots & \dots & \dots & \dots & \vdots \\ \vdots & \dots & \dots & \dots & \dots & \dots & \dots & \dots & 0 & b_i^{u1} & b_i^{u2} & b_i^{C1} & b_i^{C2} & d_i^{u1} & d_i^{u2} & d_i^{C1} & d_i^{C2} \\ \vdots & \dots & \dots & \dots & \dots & \dots & \dots & \dots & 0 & g_i^{u1} & g_i^{u2} & g_i^{C1} & g_i^{C2} & k_i^{u1} & k_i^{u2} & k_i^{C1} & k_i^{C2} \\ \vdots & \dots & \dots & \dots & \dots & \dots & \dots & \dots & 0 & m_i^{u1} & m_i^{u2} & m_i^{C1} & m_i^{C2} & n_i^{u1} & n_i^{u2} & n_i^{C1} & n_i^{C2} \\ 0 & \dots & \dots & \dots & \dots & \dots & \dots & \dots & 0 & s_i^{u1} & s_i^{u2} & s_i^{C1} & s_i^{C2} & v_i^{u1} & v_i^{u2} & v_i^{C1} & v_i^{C2} \end{bmatrix}$$

with

$$\begin{aligned}
b_i^{u_1} &= -\frac{\Delta t}{2\Delta x} \left(\bar{s} + \frac{a^2 - \bar{s}^2}{s + \bar{s}} \right)_{i-1/2}, & f_i^{u_1} &= -\frac{\Delta t}{2\Delta x} \left(\bar{s} + \frac{a^2 - \bar{s}^2}{s + \bar{s}} \right)_{i+1/2}, & d_i^{u_1} &= 1 - b_i^{u_1} - f_i^{u_1} \\
b_i^{u_2} &= -\frac{\Delta t}{2\Delta x} \left(\frac{a_2^2}{s + \bar{s}} \right)_{i-1/2}, & f_i^{u_2} &= -\frac{\Delta t}{2\Delta x} \left(\frac{a_2^2}{s + \bar{s}} \right)_{i+1/2}, & d_i^{u_2} &= -b_i^{u_2} - f_i^{u_2}, \\
b_i^{C_1} &= -\frac{\Delta t}{2\Delta x}, & d_i^{C_1} &= +\frac{\Delta t}{2\Delta x}, & f_i^{C_1} &= 0, \\
b_i^{C_2} &= -\frac{\Delta t}{2\Delta x}, & f_i^{C_2} &= +\frac{\Delta t}{2\Delta x}, & d_i^{C_2} &= 0;
\end{aligned}$$

$$\begin{aligned}
g_i^{u_1} &= +\frac{\Delta t}{2\Delta x} \left(\frac{(a_1^2 - s^2)(a_1^2 - \bar{s}^2)}{a_2^2(s + \bar{s})} \right)_{i-1/2}, & l_i^{u_1} &= +\frac{\Delta t}{2\Delta x} \left(\frac{(a_1^2 - s^2)(a_1^2 - \bar{s}^2)}{a_2^2(s + \bar{s})} \right)_{i+1/2}, & k_i^{u_1} &= -g_i^{u_1} - l_i^{u_1}, \\
g_i^{u_2} &= -\frac{\Delta t}{2\Delta x} \left(\bar{s} - \frac{a_1^2 - s^2}{s + \bar{s}} \right)_{i-1/2}, & l_i^{u_2} &= -\frac{\Delta t}{2\Delta x} \left(\bar{s} - \frac{a_1^2 - s^2}{s + \bar{s}} \right)_{i+1/2}, & k_i^{u_2} &= 1 - g_i^{u_2} - l_i^{u_2}, \\
g_i^{C_1} &= -r \frac{\Delta t}{2\Delta x}, & l_i^{C_1} &= +r \frac{\Delta t}{2\Delta x}, & k_i^{C_1} &= 0, \\
g_i^{C_2} &= -\frac{\Delta t}{2\Delta x}, & l_i^{C_2} &= +\frac{\Delta t}{2\Delta x}, & k_i^{C_2} &= 0;
\end{aligned}$$

$$\begin{aligned}
m_i^{u_1} &= -\frac{\Delta t}{2\Delta x} (a_1^2)_{i-1/2}, & q_i^{u_1} &= +\frac{\Delta t}{2\Delta x} (a_1^2)_{i+1/2}, & n_i^{u_1} &= -m_i^{u_1} - n_i^{u_1}, \\
m_i^{u_2} &= 0, & q_i^{u_2} &= 0, & n_i^{u_2} &= 0, \\
m_i^{C_1} &= -\frac{\Delta t}{2\Delta x} \left(\bar{s} + \frac{a_1^2 - \bar{s}^2}{s + \bar{s}} \right)_{i-1/2}, & q_i^{C_1} &= -\frac{\Delta t}{2\Delta x} \left(\bar{s} + \frac{a_1^2 - \bar{s}^2}{s + \bar{s}} \right)_{i+1/2}, & n_i^{C_1} &= 1 - m_i^{C_1} - q_i^{C_1}, \\
m_i^{C_2} &= -\frac{\Delta t}{2\Delta x} \left(\frac{a_1^2}{s + \bar{s}} \right)_{i-1/2}, & q_i^{C_2} &= -\frac{\Delta t}{2\Delta x} \left(\frac{a_1^2}{s + \bar{s}} \right)_{i+1/2}, & n_i^{C_2} &= -m_i^{C_2} - q_i^{C_2}
\end{aligned}$$

and

$$\begin{aligned}
s_i^{u_1} &= 0, & w_i^{u_1} &= 0, & v_i^{u_1} &= 0, \\
s_i^{u_2} &= -\frac{\Delta t}{2\Delta x} (a_2^2)_{i-1/2}, & w_i^{u_2} &= +\frac{\Delta t}{2\Delta x} (a_2^2)_{i+1/2}, & v_i^{u_2} &= -m_i^{u_1} - n_i^{u_1}, \\
s_i^{C_1} &= -\frac{\Delta t}{2\Delta x} \left(\frac{(a_1^2 - s^2)(a_1^2 - \bar{s}^2)}{a_1^2(s + \bar{s})} \right)_{i-1/2}, & w_i^{C_1} &= -\frac{\Delta t}{2\Delta x} \left(\frac{(a_1^2 - s^2)(a_1^2 - \bar{s}^2)}{a_1^2(s + \bar{s})} \right)_{i+1/2}, & v_i^{C_1} &= -s_i^{C_1} - w_i^{C_1}, \\
s_i^{C_2} &= -\frac{\Delta t}{2\Delta x} \left(\bar{s} - \frac{a_1^2 - s^2}{s + \bar{s}} \right)_{i-1/2}, & w_i^{C_2} &= -\frac{\Delta t}{2\Delta x} \left(\bar{s} - \frac{a_1^2 - s^2}{s + \bar{s}} \right)_{i+1/2}, & v_i^{C_2} &= 1 - s_i^{C_2} - w_i^{C_2}
\end{aligned}$$

where we used $s = \lambda_{ext}^+$, $\bar{s} = \lambda_{int}^+$ to lighten the notations.

Finally, it is clear that the first and last line of the system should be modified according to the considered boundary condition.

B HLL scheme applied to the Lagrangian system

With the aim of having a starting numerical scheme in the Lagrange-projection formalism, we applied the HLL strategy to the Lagrangian system (7). In particular, in order to be able to describe it and since system $\partial_t \mathbf{LQ} + \mathbf{A}(\mathbf{LQ}) \partial_\xi \mathbf{LQ} = \mathbf{S}(\mathbf{LQ}, z)$ is in non-conservative form, we first need to briefly introduce the concept of paths and path-conservative numerical schemes. Indeed, due to the presence of the non-conservative product $\mathbf{A}(\mathbf{LQ}) \partial_\xi \mathbf{LQ}$, Dirac's delta could appear in presence of discontinuities and thus we could not exploit the weak solution definition in the distributional framework. For this reason, Dal Maso, LeFloch and Murat [16] have

developed a theory to circumnavigate this problem. To this end, we first need to define a family of Lipschitz continuous paths $\Phi : [0, 1] \times \Omega \times \Omega \rightarrow \Omega$ satisfying the following regularity properties

$$\Phi(0; \mathbf{LQ}_L, \mathbf{LQ}_R) = \mathbf{LQ}_L, \quad \Phi(1; \mathbf{LQ}_L, \mathbf{LQ}_R) = \mathbf{LQ}_R, \quad \text{and} \quad \Phi(s; \mathbf{LQ}, \mathbf{LQ}) = \mathbf{LQ}.$$

Then, given a function \mathbf{LQ} with bounded variation, the non-conservative product $\mathbf{A}(\mathbf{LQ})\partial_\xi \mathbf{LQ}$ would make sense as a locally bounded measure. For more details, refer for instance to [6, 18]. Obviously, a further difficulty is related to the choice of the path. Here we do not focus on such a problem and we simply exploit the easiest formulation for the definition of the path, namely the straight segment,

$$\Phi(s; \mathbf{LQ}_L, \mathbf{LQ}_R) = \mathbf{LQ}_L + s(\mathbf{LQ}_R - \mathbf{LQ}_L).$$

Moreover, it is important to underline that, due to the numerical viscosity of the method, even if the "correct" path is chosen, the numerical output could converge to the wrong solution and not the physical one [6].

Then, once the family of paths has been chosen, considering system (7) in compact form $\partial_t \mathbf{LQ} + \mathbf{A}(\mathbf{LQ})\partial_x \mathbf{LQ} = \mathbf{0}$ and flat topography, the general path-conservative formula reads

$$\mathbf{LQ}_i^{n+1} = \mathbf{LQ}_i^n - \frac{\Delta t}{\Delta x} (\mathbf{D}_{i+1/2}^- + \mathbf{D}_{i-1/2}^+)$$

where $\mathbf{D}_{i+1/2}^\pm = \mathbf{D}^\pm(\mathbf{LQ}_i, \mathbf{LQ}_{i+1})$ are two continuous functions satisfying

$$\mathbf{D}^\pm(\mathbf{LQ}, \mathbf{LQ}) = 0 \quad \forall \mathbf{LQ} \in \Omega$$

and

$$\mathbf{D}^-(\mathbf{LQ}_L, \mathbf{LQ}_R) + \mathbf{D}^+(\mathbf{LQ}_L, \mathbf{LQ}_R) = \int_0^1 \mathbf{A}(\Phi(s; \mathbf{LQ}_L, \mathbf{LQ}_R)) \frac{\partial \Phi}{\partial s}(s; \mathbf{LQ}_L, \mathbf{LQ}_R) ds$$

Once again, here we do not give further details about path-conservative schemes but we simply refer to [18] and the references therein.

In particular, here we briefly show the interpretations of the HLL scheme as a PVM (Polynomial Viscosity Matrix) method and we directly refer to [6] for more details. Therefore, considering the following polynomial $P(x) = \alpha_0 + \alpha_1 x$ with coefficients

$$\alpha_0 = \frac{\lambda_{ext}^+ |\lambda_{ext}^-| - \lambda_{ext}^- |\lambda_{ext}^+|}{\lambda_{ext}^+ - \lambda_{ext}^-}, \quad \alpha_1 = \frac{|\lambda_{ext}^+| - |\lambda_{ext}^-|}{\lambda_{ext}^+ - \lambda_{ext}^-},$$

we obtain the following final form for the fluctuations

$$\mathbf{D}_{i+1/2}^\pm = \frac{1}{2} \left(\mathbf{A}_{i+1/2}(\mathbf{LQ}_{i+1} - \mathbf{LQ}_i) \right) \pm \frac{1}{2} P_{i+1/2}(\mathbf{A}_{i+1/2}) (\mathbf{LQ}_{i+1} - \mathbf{LQ}_i)$$

or equivalently

$$\mathbf{D}_{i+1/2}^\pm = \frac{1}{2} \left(\mathbf{A}_{i+1/2}(\mathbf{LQ}_{i+1} - \mathbf{LQ}_i) \right) \pm \frac{1}{2} \left(\alpha_{0,i+1/2} (\mathbf{LQ}_{i+1} - \mathbf{LQ}_i) + \alpha_{1,i+1/2} \mathbf{A}_{i+1/2}(\mathbf{LQ}_{i+1} - \mathbf{LQ}_i) \right).$$

Recalling that $\mathbf{A}(\mathbf{LQ}) = \frac{\partial \mathbf{F}(\mathbf{LQ})}{\partial \mathbf{LQ}} + \mathbf{B}(\mathbf{LQ})$, we can also express the fluctuations as

$$\begin{aligned} \mathbf{D}_{i+1/2}^\pm &= \frac{1}{2} \left(\mathbf{F}(\mathbf{LQ}_{i+1}) - \mathbf{F}(\mathbf{LQ}_i) + \mathbf{B}_{i+1/2}(\mathbf{LQ}_{i+1} - \mathbf{LQ}_i) \right) \pm \\ &\pm \frac{1}{2} \left(\alpha_{0,i+1/2} (\mathbf{LQ}_{i+1} - \mathbf{LQ}_i) + \alpha_{1,i+1/2} \left(\mathbf{F}(\mathbf{LQ}_{i+1}) - \mathbf{F}(\mathbf{LQ}_i) + \mathbf{B}_{i+1/2}(\mathbf{LQ}_{i+1} - \mathbf{LQ}_i) \right) \right). \end{aligned}$$

Moreover, since in our case $\lambda_{ext}^- = -\lambda_{ext}^+$, it is clear that we always have $\alpha_1 = 0$.

Finally, it is straightforward to include the topography source term in the numerical method. Indeed, few computations give us

$$\begin{aligned} \mathbf{D}_{i+1/2}^{\pm} &= \frac{1}{2} \left(\mathbf{A}_{i+1/2} (\mathbf{LQ}_{i+1} - \mathbf{LQ}_i) - \mathbf{S}_{i+1/2} (z_{i+1} - z_i) \right) \pm \\ &\pm \frac{1}{2} P_{i+1/2} (\mathbf{A}_{i+1/2}) \left((\mathbf{LQ}_{i+1} - \mathbf{LQ}_i) - \mathbf{A}_{i+1/2}^{-1} \mathbf{S}_{i+1/2} (z_{i+1} - z_i) \right). \end{aligned}$$

In practice, we exploit the following formula

$$\begin{aligned} \mathbf{D}_{i+1/2}^{\pm} &= \frac{1}{2} \left(\mathbf{F}(\mathbf{LQ}_{i+1}) - \mathbf{F}(\mathbf{LQ}_i) + \mathbf{B}_{i+1/2} (\mathbf{LQ}_{i+1} - \mathbf{LQ}_i) - \mathbf{S}_{i+1/2} (z_{i+1} - z_i) \right) \pm \\ &\pm \frac{1}{2} \left(\alpha_{0,i+1/2} (\mathbf{L}\tilde{\mathbf{Q}}_{i+1} - \mathbf{L}\tilde{\mathbf{Q}}_i) + \alpha_{1,i+1/2} \left(\mathbf{F}(\mathbf{LQ}_{i+1}) - \mathbf{F}(\mathbf{LQ}_i) + \mathbf{B}_{i+1/2} (\mathbf{LQ}_{i+1} - \mathbf{LQ}_i) - \mathbf{S}_{i+1/2} (z_{i+1} - z_i) \right) \right) \end{aligned}$$

with $\mathbf{L}\tilde{\mathbf{Q}} = (L_1, L_1 h_1, L_1 h_1 u_1, L_2, L_2 h_2 + z, L_2 h_2 u_2)^t$.